
Article:
Nejat, P., Calautit, J.K., Majid, M.Z.A. et al. (3 more authors) (2016) Evaluation of a two-sided windcatcher integrated with wing wall (as a new design) and comparison with a conventional windcatcher. Energy and Buildings, 126. pp. 287-300. ISSN 0378-7788

https://doi.org/10.1016/j.enbuild.2016.05.025

Evaluation of a two-sided windcatcher integrated with wing wall (as a new design) and comparison with a conventional windcatcher

Payam Nejat[1], John Kaiser Calautit[2], Muhd Zaimi Abd. Majid[3] , Ben Richard Hughes[2], Iman Zeynali [4,5], Fatemeh Jomehzadeh[1]

1: Faculty of Civil Engineering, Universiti Teknologi Malaysia, UTM- Skudai, Johor, Malaysia

Payam.nejaat@gmail.com, Tel: +6075536508, Fax: +6075537843

2: Department of Mechanical Engineering, University of Sheffield, Sheffield, UK

3: Construction Research Center, Construction Research Alliance, Universiti Teknologi Malaysia, Skudai, Johor, Malaysia

4: Faculty of Engineering, Ferdowsi University of Mashhad, Iran

5: Asia Building and Environment Research (ABER) center, Iran

Abstract

In buildings, 60% of energy consumption is associated to HVAC systems. One solution to reduce this share is the application of natural ventilation systems. Windcatcher and wing wall are two well-known techniques for natural ventilation which have been used in different regions. Nevertheless, in areas with low wind speed such as tropical climate of Malaysia there is hesitation for application of natural ventilation systems. The integration of windcatcher with wing wall can potentially enhance the ventilation performance. However, this configuration was not looked into by pervious investigations; thus, this study aims to address this gap of research by evaluating: first, the effect of wing wall angle on the ventilation performance; second, comparethe performance of this new design with a conventional windcatcher. This research had two main investigative steps: experimental scaled wind tunnel testing and CFD simulation. Four reduced-scale models of two-sided windcatcher were tested in a low speed wind tunnel. Three models were integrated with wing wall in 30°, 45° and 60° incident angles and the another windcatcher was a conventional two-sided windcatcher, which is typical in regions with predominant wind direction. The CFD validation against experiment showed a good agreement. The best operation was observed in the windcatcher with 30° wing wall angle which could supply 910 l/s fresh air into the room in 2.5 m/s wind speed. Hence, the new design had 50% more ventilation performance comparing with conventional two-sided windcatcher in the same external wind speed. Finally, it was concluded that this new design can satisfy requirements of ASHRAE 62.1.

Keywords: Windcatcher, natural ventilation, wing wall, passive cooling, CFD

1. Introduction

Buildings are responsible for 40% of the global energy consumption and accounts for around 40-50% of the carbon emissions all over the world [1]. Moreover, almost two-thirds of total energy consumption in buildings is used for space heating, ventilating, and air conditioning (HVAC) systems [2]. Generally, less energy use for HVAC systems is required but without compromising a comfortable and healthy indoor environment [3]. In this regard, one promising solution that has gained attention is incorporating free and natural resources from nature such as natural ventilation [4]. Recently, natural ventilation techniques such as windcatchers are increasingly being employed in new buildings for increasing the fresh air rates and reducing the energy consumption [2] and [5].

A windcatcher can be defined as an architectural element placed on the building roof [6] which provides fresh air to the interior living spaces and release stale air through windows or other exhaust segments [7]. Traditionally, countries in Middle East such as Iran, Iraq, Qatar and Emirates as well as North African region like Egypt and Algeria have utilized windcatcher for the past three thousand years [8]. Generally, the windcatcher systems employs both ventilation principles of wind driven and stack effect [9]. The first one works on the wind pressure difference between the windcatcher's inlet and outlet which are usually sufficient to drive air into the room, and remove warm and stale inside air out [10]. Moreover, windcatcher can direct airflow through the channel, while there have been temperature variation between indoor and outdoor space, this mode is known as stack effect [11]. Bahadori et al. [12] stated that the main benefit of windcatcher, like other passive technologies, is that it exploits wind renewable energy for their operation so they are considerably cost effective and more healthier. In addition to improving human comfort, they have low maintenance cost due to having no moving parts, exploit clean and fresh air at roof level compared to low level windows [13]. Generally, windcatchers are classified in five groups of one-sided, two-sided, four, six and eight-sided with respect to the number of the openings. Based on the study [7], the efficiency of the two-sided is higher than other types, particularly in zero wind incident angle, which can induce the most volume of air flow into the room. Hence, this type is a typical conventional windcatcher in regions with predominant wind direction [14] and [15].

Beside the windcatcher, wing wall is another architectural element for natural ventilation to direct the external air flow into the building by projecting portions of the walls vertically from the openings [16]. Broadly, the ventilation rate can be improved by wing wall application owing to creation of pressure differences. For instance, Khan et al. [10] reported that the average air velocity in the room with wing wall is 40% of the outdoor wind speed while without winging wall it is only 15%. Fig. 1 illustrates the provision of wing wall in a building facade vertically between two openings [17].

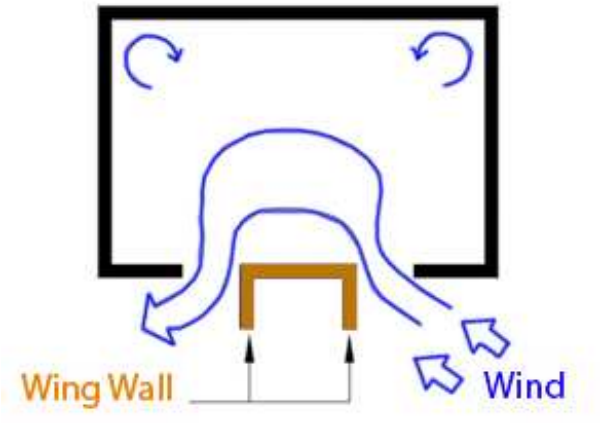

Figure 1. The illustration of wing wall applied for natural ventilation enhancement in building [17].

Despite all advantages of windcatcher, this passive cooling system has less efficiency in low wind speed conditions because the wind driven force is the primary driving force for the windcatcher [15]. For this reason, most of the pervious investigations studied windcatcher in medium to high wind speed (3 to 5 m/s) conditions such as [18] and [19]. Therefore, in some regions where the speed of ambient wind is low (e.g. tropical climate of Malaysia), windcatcher cannot be implemented efficiently and the numbers of windcatcher studies in this climate are very limited.

In contrast, wing walls can be very effective in situations with low wind speed and variable directions [20]. Thus, the combination of windcatcher with wing wall can potentially improve the natural ventilation rates in low wind speed conditions. Hence, the current study introduces a new design consisted of a two-sided windcatcher (due to predominant wind direction in Malaysia climate) integrated with wing walls, called here TWIW (two-sided windcatcher integrated with wing walls). Therefore, the current research has two main objectives including:

- First, to study the effect of wing wall angle on the ventilation performance of the windcatcher and find the optimum angle which shows the best ventilation performance (based on the supply airflow rates) in low wind speed climate such as Malaysia.
- The secondobjective isto compare the TWIW with aconventional two-sided windcatcher (CTSW).

2. Literature review

Different researchers studied the ventilation performance of two-sided windcatcher as well as other types of windcatcher by wind tunnel testing and numerical method [5], [21] and [14]. In addition, few investigations evaluated the performance of wing wall –alone– for natural ventilation. In this section a brief review of related pervious researches are summarized.

Afshin et al. [5] investigated ventilation performance of a two-sided windcatcher for different wind angles (α from 0° to 90°) by wind tunnel experiment. A 1:50 reduced-scale model of a conventional two-sided windcatcher in the city of Yazd (Iran) was modeled. The results demonstrated that the transition angles of the house window and windward opening for all wind velocities occurred at the wind angles of 39° and 55°, respectively. Based on results, it was concluded that the windcatcher performed as a chimney when wind angle was greater than the windward transition angle (α = 55°) and the highest ventilation rate was seen when the wind was perpendicular to the windcatcher opening.

Montazeri et al. [14] studied the performance of natural ventilation in a reduced-scale model (1:40) of two-sided windcatcher system. For various air incident angles, the pressure coefficients of all surfaces of the model and volumetric airflow were measured in an open-circuit wind tunnel. Moreover, to validate the accuracy, the research developed analytical and numerical CFD models of the experimental setup and satisfying agreement among the results was observed. It was established that in higher incident angles of the wind, short-circuiting emerges in the windcatcher and reaches the maximum at wind incident angle of 60. The study highlighted the capacity of the two-sided wind catcher for improving the natural ventilation inside dwellings. The results of comparison factor for one and two-sided wind catcher pointed out that the one-sided windcatcher is more suitable in regions with predominant wind direction.

Haw et al. [21] assessed the ventilation performance of a windcatcher with a Venturi shaped roof (for providing considerable negative pressure to induce air movement) in hot and humid climate, Malaysia using CFD and experimental methods. The obtained results showed that at a low outside air velocity of 0.1 m/s, the windcatcher was capable of supplying airflow at 57 air changes per hour (ACH) inside the building. Moreover, the indoor air velocity was observed to be between the range of 0.05 m/s and 0.45 m/s. The study demonstrated the capability of a windcatcher in achieving adequate indoor air quality and enhancing thermal comfort of the inhabitants under hot and humid climate.

Givoni [22] carried out the first investigation of the effect of wing wall on natural ventilation performance of room models with two lateral openings. According to obtained results of the wind tunnel test, he concluded that the wing wall had high potential to increase the air speed inside the room. Later Mak et al. [17] used numerical CFD technique to validate the experimental results of Givoni's study. Three different room configurations with and without wing walls at varying wind directions were modeled. The simulation results were generally in good agreement with Givoni's experimental measurements and confirmed that both air change per hour and the average air velocity inside the room are increased by installation of wing walls. The wing wall at the air incidence angle of around 45° showed the best ventilation performance. Furthermore, the highest value of the percentage of mean indoor air speed to outdoor wind speed (20%) occurred at an angle of 45°.

Moreover, Chungloo and Tienchutima [23] conducted CFD analysis to study the effect of integrating wing wall with a balcony on the wind speed distribution inside the room at varying wind directions (0°-90°). The computational results pointed out that the wing wall was able to improve the ventilation performance especially at a range of 30° to 75° wind angles; however, the balcony reduced the ventilation by 40-55%.

3. **From the review of literature, it can be concluded that although different studies have been conducted on windcatcher and wing wall, there is no study that investigated the integration of windcatcher with wing wall. Therefore, the aim of this research is to address the gap of current studies by evaluating the effect of wing wall angle on the ventilation performance of the TWIW and alsocompare TWIW with the CTSW. Furthermore, two-sided windcatchers are typically analysed by previous works [5, 14] using uniform flow profiles which does not take into account the frictional drag of the ground surface which generates a boundary layer in which there is a progressive reduction in wind speed towards the ground. Therfore, this study will carry out simulations of the two-sided windcatcher in an atmospheric boundary layer (ABL) flow to address this gap in literature.Research methodology**

This research employedtwo investigative methods: experimental and computational fluid dynamics (CFD) study. Previous studies proved that tthese methods are reliablein terms of evaluating the ventilation performance and efficiency of wind catchers [9] . The experiment can be done in either full-scale or reduced-scale wind tunnel test. Like many previous works that assessed the windcatcher, thewind tunnel test was selected for the experimental study because a controllable environment was necessary to study the effect of different flow speeds and also due to the lower cost. In addition, the reduced-scale model can predict the behavior of the flow same as the full scale model provided that the similarity in geometry and Reynolds number are achieved [24]. Both of these research methods are explained in the following sections in details.

3.1 Experimental procedure and wind tunnel set-up

In aerodynamic research, the Reynolds number determines the patterns of air flow around a building and the related wind loads. Thus, the reduced-scale model tested in wind tunnel should ideally experience the same Reynolds number exactly as the actual case in a real environment [2,14,24]. Nevertheless, even in very large wind tunnels which can run at high wind speeds, it is usually difficult to simulate scaled models at exactly similar Reynolds number as it will be in a full scale environment [2]. But, if the Reynolds number is not less than 10,000, the similarity of Reynolds number for the model and real object for sharp edges of model is negligible because flow separation occurs fixedly in these sharp points regardless of Reynolds number and thus, the wind reaction is nearly independent from Reynolds number [2]. In this study it was ensured that Reynolds number value was above the acceptable range by running the wind tunnel at 10 m/s.

One of the potential challenging issues of wind tunnel testing is blockage which can be defined as model frontal area over test section cross-sectional area. It is suggested to select suitable scaling factor that can achieve blockage of less than 5% [25]. Modelswith relative dimensions larger than this would force the air flow to be squeezed between the model and wind tunnel walls in an unrealistic manner which require blockage corrections [2,7] and [25]. Therefore, to avoid the above matter with considering test section area and model cross-sectional area, the model was scaled down by 1:10 to achieve a blockage less than 5%.

The reduced-scale models were made from Plexiglas with a thickness of 5 mm. The Plexiglas sheets were cut by laser with accuracy of 0.001 mm to achieve high accuracy. As shown in Fig.2 and Fig.3, the reduced-scale models are composed of a rectangular cuboid with 600 mm length, 400 mm width and 300 mm height (representing a small class room) and a two-sided windcatcher integrated with wing walls. The windcatcher consisted of two channels which were separated with internal partition wall with 5 mm thickness. The heights of windcatcher and wing walls were 150 mm. The justification for the height selection is the fact that the height of traditional windcatchers are mostly between 1.5 m to 3 m and modern windcatchers are shorter than traditional ones for better adoption with current buildings [26].

The size of openings and cross-sections of windcatcher were 100 mm by 100 mm. The justification of the size of opening was based on typical size as described in the references [11] and [27]. Three models were similar but with different wing wall angle of α (angle of wing wall against wind direction). Angle of α consisted of 30°, 45° and 60° and the shading device lengths –A– were 155 mm ,188 mm and 205 mm respectively.

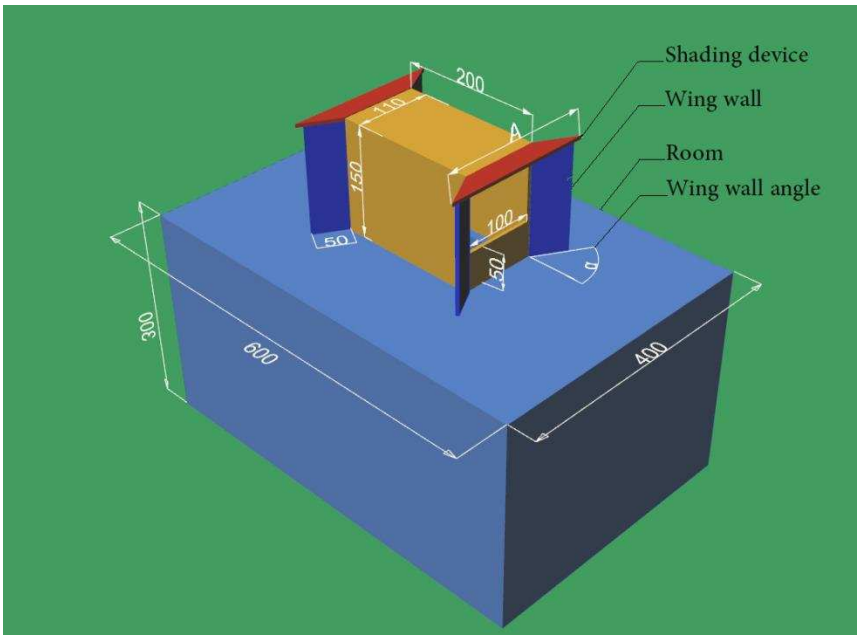

Figure 2. The schematic of model including room, windcatcher, wing walls and shading devices (all dimensions were same for all models except the angle of α and A the length of shading device).

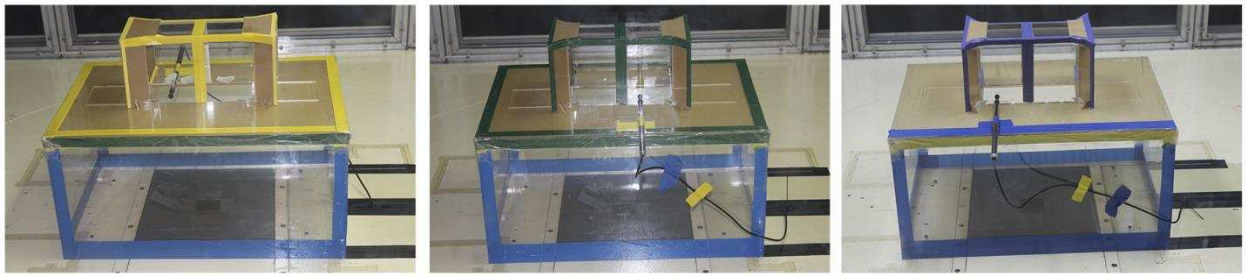

Figure 3. The three reduced-scale TWIW models during the airflow measurement with a hot wire in the supply/exhaust channel (from left to right α=30°, α=45° and α= 60°).

The CTSW has similar geometry to TWIW (Fig.4) but with internal louvers in openings because louvers are a common component of the new conventional windcatchers [15]. The number and angle of the louvers were 6 and 35° which were selected based on the optimum as detailed in references [19] and [28].

Figure 4. conventional windcatcher (CTSW) model during airflow measurements.

The experiment was conducted in the Low Speed Wind Tunnel (UTM-LST) of University Technology Malaysia (UTM). This wind tunnel is one of the most equipped and largest in the south East Asia as well as a member of Subsonic Aerodynamics Testing Association. The wind tunnel is a closed-circuit, horizontal return wind tunnel with a rectangular test section of 2 m (W) * 1.5 m (H) * 5.8 m (L). The test section pressure is atmospheric with a maximum wind speed of 80 m/s (Fig. 5).

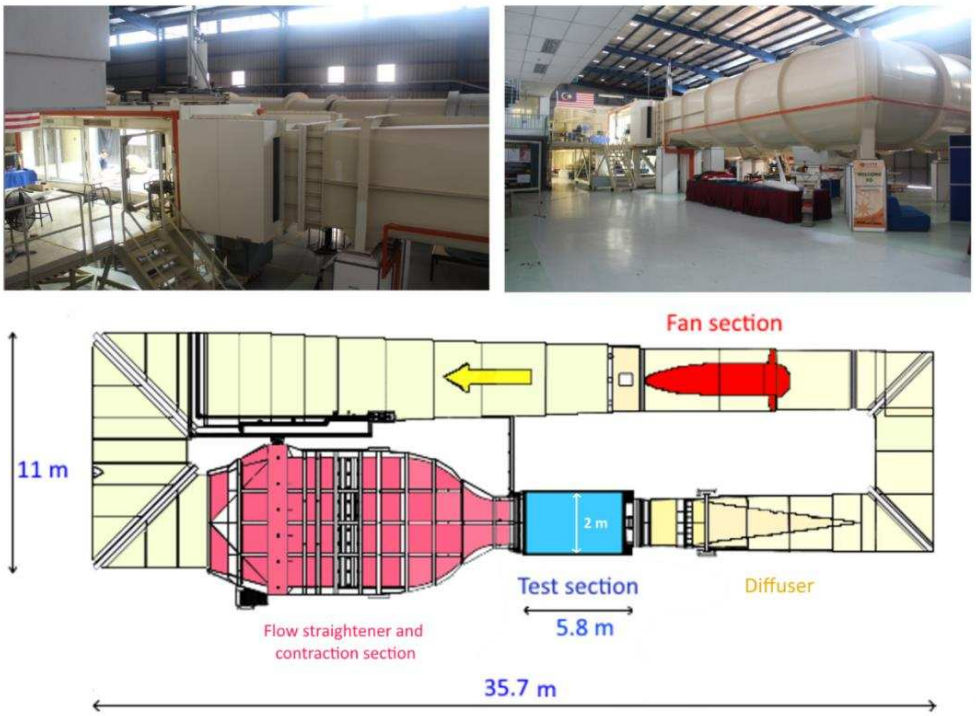

Figure 5. The wind tunnel of University Technology Malaysia and its plan with dimensions.

Based on the winddata of Malaysia, the predominant directions of the wind were northeast and southwest with an average of 2.5 m/s [29], [30] and [31]. Therefore, with respect to scale number of 1:10, the wind speed in wind tunnel should be set to 25 m/s to achieve the same Reynolds number. However, due to safety and strength of models, the wind speed was adjusted to 10 m/s.

The tests were based on the assessment of the windcatcher's ability to provide fresh air (air flow rate in inlet diffuser) and extracting stale air from room (air flow rate in outlet diffuser). Therefore, air velocity was measured in six points (I_1−I_6) in inlet diffuser and six points (E_1−E_2) in outlet diffuser.

In order to place the sensor inside the channel, two holes were drilled on supplychannel as well as exhaust channelof the windcatcher (same level with roof of the room). The test consisted of 12 steps of data recoding for each model (totally 48). As shown in Fig. 6, points (I_1−I_6) and (E_1−E_2) are positioned in symmetric grid in horizontal plane (parallel to roof) in of supplyand exhaustt channel. For each point, the measurement was done in Z vertical direction (parallel to channel) with duration of 1 minute which was repeated 3 times to have a more reliable data.

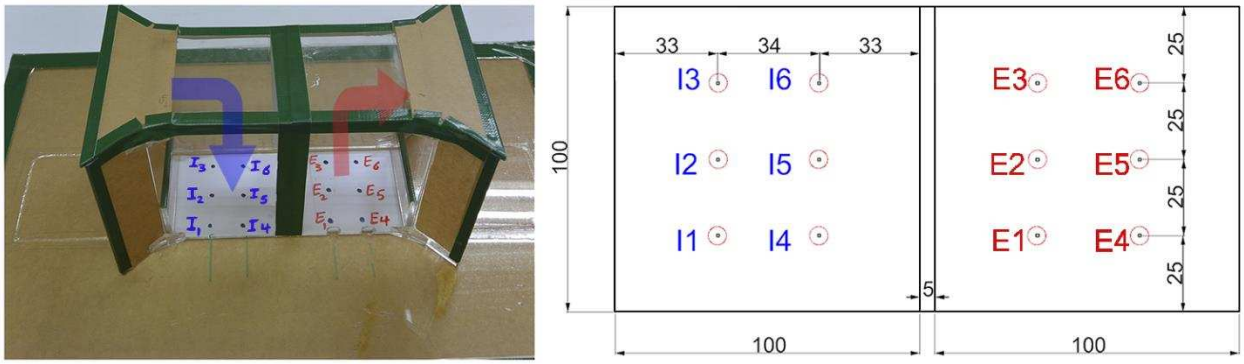

Figure 6. The positions of I and E points in inlet and outlet diffuser of models (all the dimensions are in mm).

The method used for air velocity measurement was Constant Temperature Anemometry (CTA). The air velocity data logger utilized in this investigation was an OMEGA® HHF-SD1 combination standard thermistor anemometer and a hot wire which had multiple features that was required in this study. The OMEGA® HHF-SD1 hadan accuracy of 5% of reading and resolution of 0.01 m/s. The hot wire sensor had 4 µm diameter, 1.27 mm long and can measure mean and fluctuating velocities in one-dimensional flows.

The experimental uncertainly was calculated by the method of Kline and McClintock [32]. The maximum uncertainly in velocity number was 4.2%. During the experiment, it was ensured that there was no or minimal variation of the flow thermal and hydro-dynamical properties before conducting measurements. Therefore, the uncertainly due to variation of thermos-physical properties was assumed to have minimal effect on accuracy of the measurements. The details of the uncertainly analysis and results are presented in Appendix I. The summary of experimental procedure is presented in Table 1.

Table 1. The summary of experimental procedure.

Experiment summary	
Material of models	**0.5cm Plexiglas, cut with laser**
Number of models	**3 TWIW** **1 CTSW**
Scale of the model	**1:10**
Speed of wind	**10 m/s**
Date	**October 2015, 3 days**
Measurement factor	**Air velocity**
Type of sensor	**OMEGA® HHF-SD1**
location	**UTM Aero lab**
Wind tunnel specifications	**Low speed, test section :** **2 m * 1.5 m * 5.8m**

3.2 Computational Fluid Dynamics (CFD) modelling

The computational domain used in this study for simulating atmospheric boundary layer (ABL) flows around different types of windcatcher configurations is illustrated in Fig.7. The domain size and location of model were based on the guideline of COST 732 [33] for environmental wind flow studies. The COST 732 suggested that for a single building with height of H, the lateral extension of the domain should be 5H (the distance between building's sidewalls and the lateral boundaries of the computational domain). For extensionof the domain in flow direction, 5H was recommended for inlet. For the outlet, the boundary should be positioned at least 15H behind the building to allow the flow to re-develop behind the wake region, as fully developed flow is normally assumed as the boundary condition in steady RANS calculations. For the vertical extension of the domain, COST 732 advised between 4H and 10H with considering the effect of blockage. So in this study, 10H was selected to minimize the effect of the blockage [33].

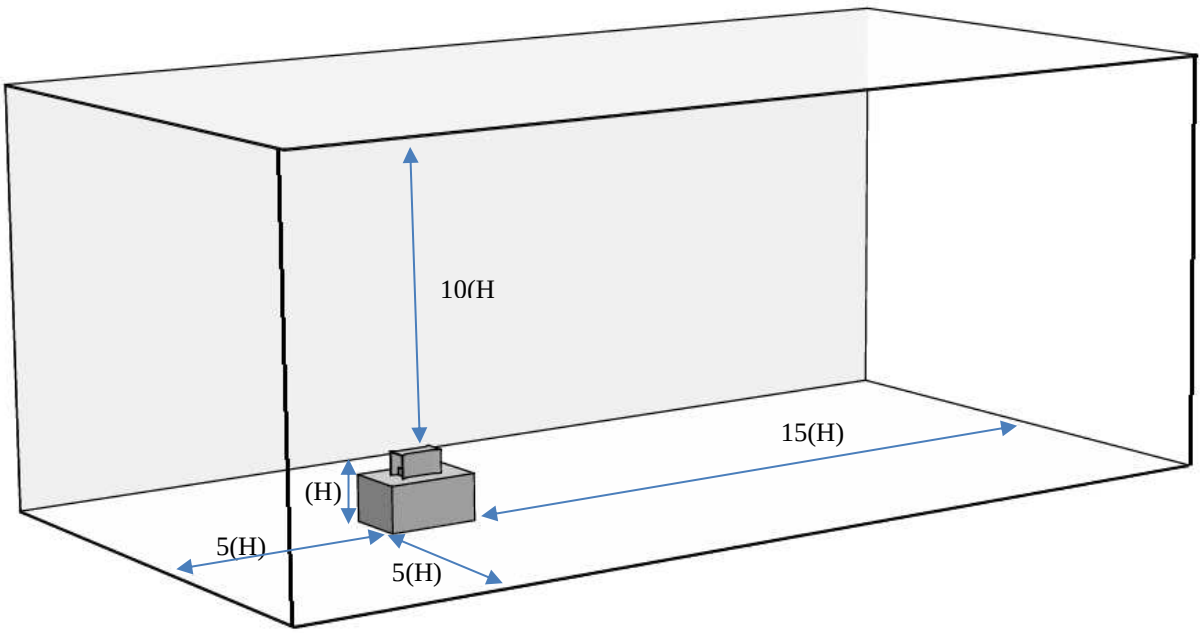

Figure 7. The computational domain for the ABL flow simulations.

The CFD simulation consisted of three phases. First phase was conducted for the validation of numerical method, which in this phase the wind speed was set to 10 m/s, same as the experimental procedure. Second phase included investigation about effect of different wing wall angles (α in Fig. 2) on the ventilation performance, which in this phase the wind speed was set to simulate the average of Malaysia wind speed (2.5 m/s). After finding the optimum α from the previous step, in the final phase, the ventilation performance of the TWIW wascompared with CTSW in different outdoor wind speeds.

The three-dimensional and steady Reynolds-Averaged Navier-Stokes (RANS) computations were performed using the commercial CFD code FLUENT 14.5 to solve the flow equations. The computational model employed the control volume method and the Semi-Implicit Method for Pressure-Linked Equations (SIMPLE) velocity-pressure coupling algorithm with the second order upwind discretization. Based on the turbulence model analysis, the standard k- ε model was used as the turbulence model (see the details in section 3.2.4.2). The use of the standard k- ε model on natural ventilation studies was also found in previous works of [34] and [35] to be reliable and accurate. The governing equations and its derivations werenot included here but can be found in the ANSYS 14.5 Fluent theory guide [36].

3.2.1 Mesh generation

The computational volumes were applied with non-uniform mesh due to the complexity of the geometry shape. The meshed model comprised of 1,514,234 nodes and 8,138,056 elements. As observed in Fig. 8, the mesh around the wind catcher and openings were refined to ensure that the flow field was accurately captured in the simulations. The mesh was based on a grid sensitivity and flux balance analysis that will be described in Section 3.2.4.2.

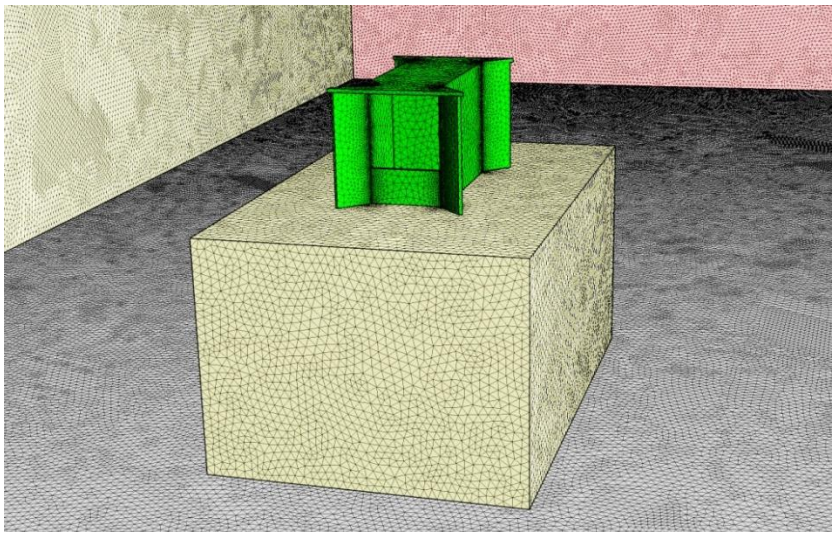

Figure 8. Mesh generation on the computational model.

3.2.2 Solution convergence and flux balance

There are no common metrics for deciding solution convergence. Residuals that are useful for one type of simulation are sometimes misrepresentative for other types of simulations. Therefore it is important to decide solution convergence not only by investigative residual levels, but also by monitoring relevant variables [36]. In this study, the convergence of the solution (Fig. 9a) and relevant variables such as inflow and outflow velocities (Fig. 9b) were monitored and the solution was completed when there were no changes between iterations. In addition to monitoring residuals and solution variables, the property conservation was also checked if achieved. This was carried out by performing a mass flux balance for the converged solution. This option was available in the FLUENT flux report panel which allows computation of mass flow rate for boundary zones. For the simulation of wind tower, the mass flow rate balance was below the required value or <1% of smallest flux through domain boundary (inlet and outlet).

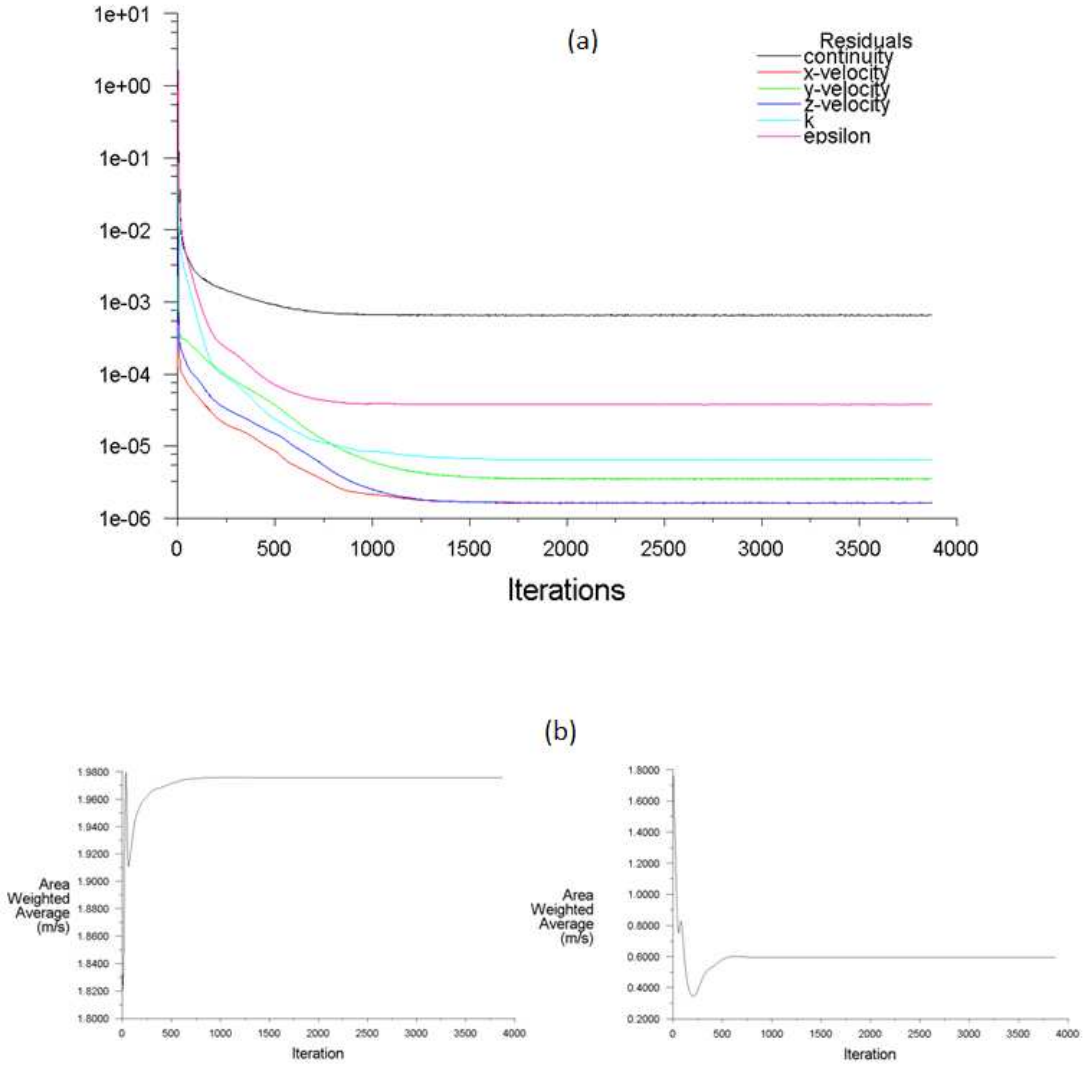

Figure 9. (a) Convergence and (b) solution monitoring.

3.2.3 Boundary conditions

The boundary conditions were specified according to guidelines of AIJ [37] and COST 732 [33]. The profiles of the airflow velocity U (Fig. 10a) and turbulent kinetic energy k (Fig. 10b) were imposed at the inlet which were based on [38], with the streamwise velocity of the approaching flow obeying the power law with an exponent of 0.25 which corresponds to a sub-urban terrain. The values of ε for the k-epsilon turbulence models were acquired by assuming local equilibrium of $P_k = \varepsilon$ [33]. The standard wall functions [39] were applied to the wall boundaries except for

the bottom wall or ground, which had its wall functions adjusted for roughness [40]. According to [40], this should be specified by an equivalent sand-grain roughness height k_s and a roughness constant C_s. The horizontal non homogeneity of the ABL was limited by adapting sand-grain roughness height and roughness constant to the inlet profiles, following the equation of [41]:

$$k_s = \frac{9.793 z_0}{C_s}$$

Where z_0 is the aerodynamic roughness length of the sub-urban terrain. The values selected for sand-grain roughness height and a roughness constant 1.0 mm and 1.0 [38]. The sides and the top of the domain were established as symmetry boundary conditions, indicating zero normal velocity and zero gradients for all the variables at the side ant top wall. At the outlet boundary wall, zero static pressure was used. Summary of the boundary conditions are shown in Table 2.

Table 2. Summary of boundary conditions for the domain

Parameter	Domain 2 (ABL)
Micro-Climate	Fluid zone
Walls	Top: Symmetry Side: Symmetry Bottom: Wall
Macro-climate	Fluid zone
Operating Pressure	Atmospheric
Viscous Model	k- ε (standard)
Near-Wall Treatment	Standard wall functions
Velocity Inlet	ABL Profile (Figure 11)
Pressure Outlet	0 Pa
Solver Type	Pressure-based
Time	Steady
Gravity	**-9.81 m/s^2**

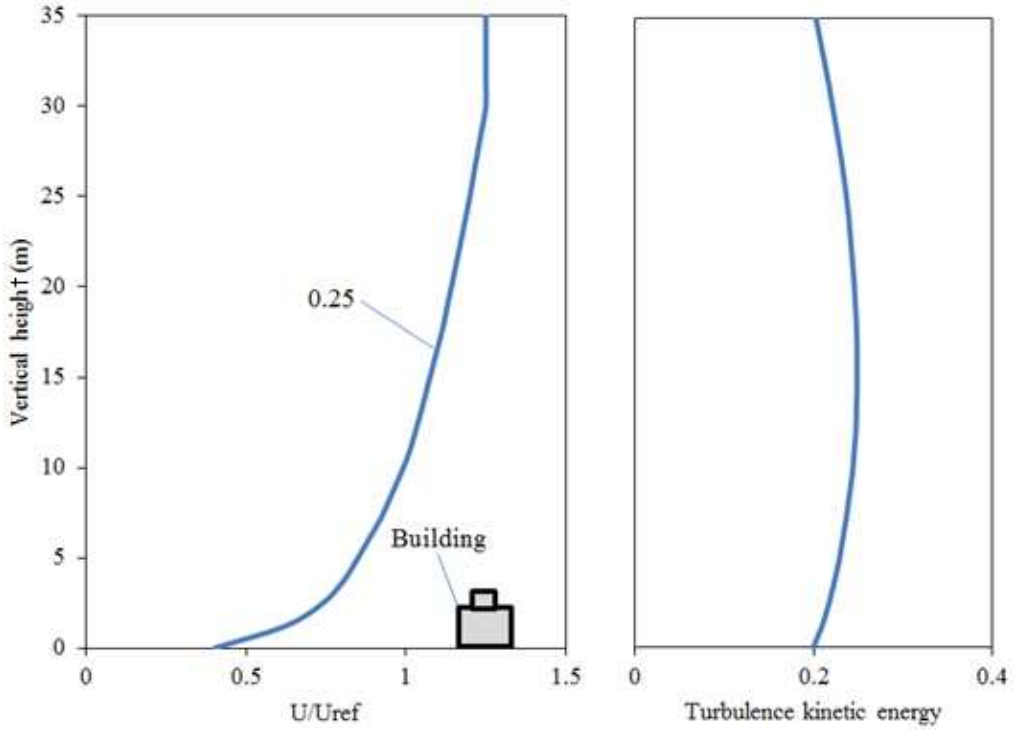

Figure 10. (a) ABL flow profile (b) turbulence kinetic energy profile of the approach flow.

3.2.4 Sensitivity analysis

3.2.4.1 Grid adaption

In order to ensure that the numerical model wasindependent from the grid size, different number of grids were evaluated. The computational mesh used was based on a mesh sensitivity analysis which was performed by conducting additional simulations of the same domain and boundary conditions but with various mesh sizes. The area-weighted average value of the inflow velocity was taken as the error indicator (Fig. 11), as the grid was refined from 4,789,021 to 10,254,352 elements. The discretization error was found to reduce to below 1% when the cells were increased 8,138,056 and hence the size was used in this investigation. The repetition of numerical model with finer mesh had no considerable effects on the results. Therefore, it could be concluded, using the mentioned mesh size was accurate and no need for the finer mesh.

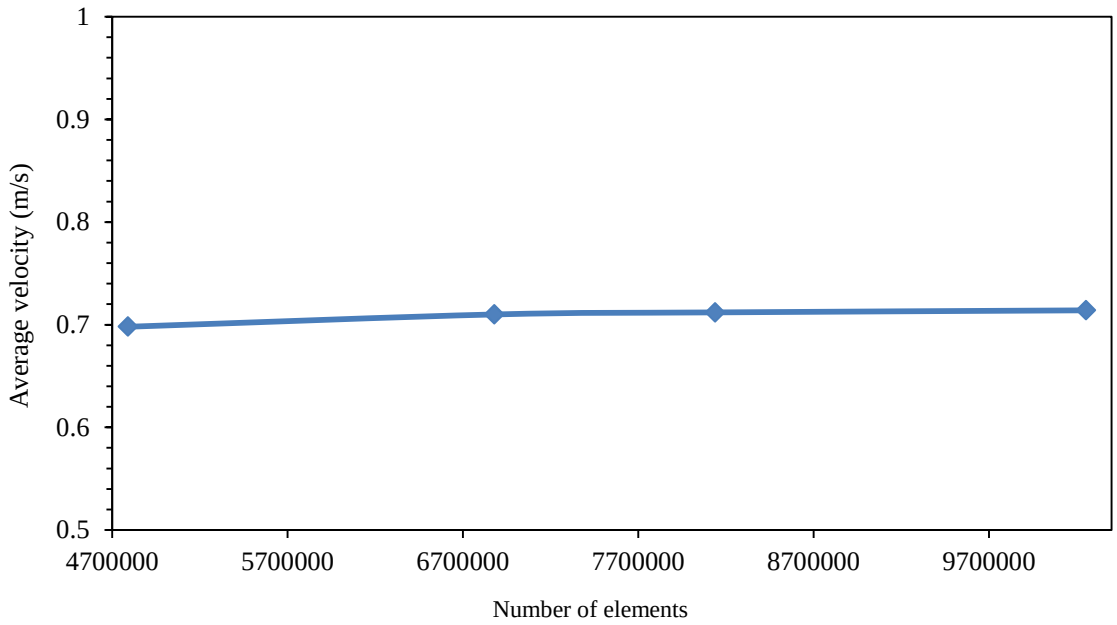

Figure 11. Mesh sensitivity analysisof the airflow supply velocity,

3.2.4.2 Sensitivity of turbulence model

Turbulence model validation is of fundamental importance for the reliability of CFD simulations.The objective of turbulence sensitivity analysis wasto verify that the selected turbulence model wasable to present the most accurateprediction of the flow. For this reason, three turbulence models were evaluated including (1) the standard k-ε (Sk-ε) model, (2) the realizable k-ε (Rk-ε) model and (3) the renormalization group k-ε model (RNG k-ε). The predictions of the three different turbulence models on the airflow velocity in I and E points of inlet and outlet channels of TWIW with α of 30° are illustrated in Fig. 12 and Table. 3. The standard k-ε model clearly provided the best agreement with the experimental data. The average of difference between experimental data and mentioned model was 11% (lower than the other two models). Therefore, standard k-ε model was selected for current numerical study which was in agreement with pervious windcatcherstudies in reference of [34] and [35].

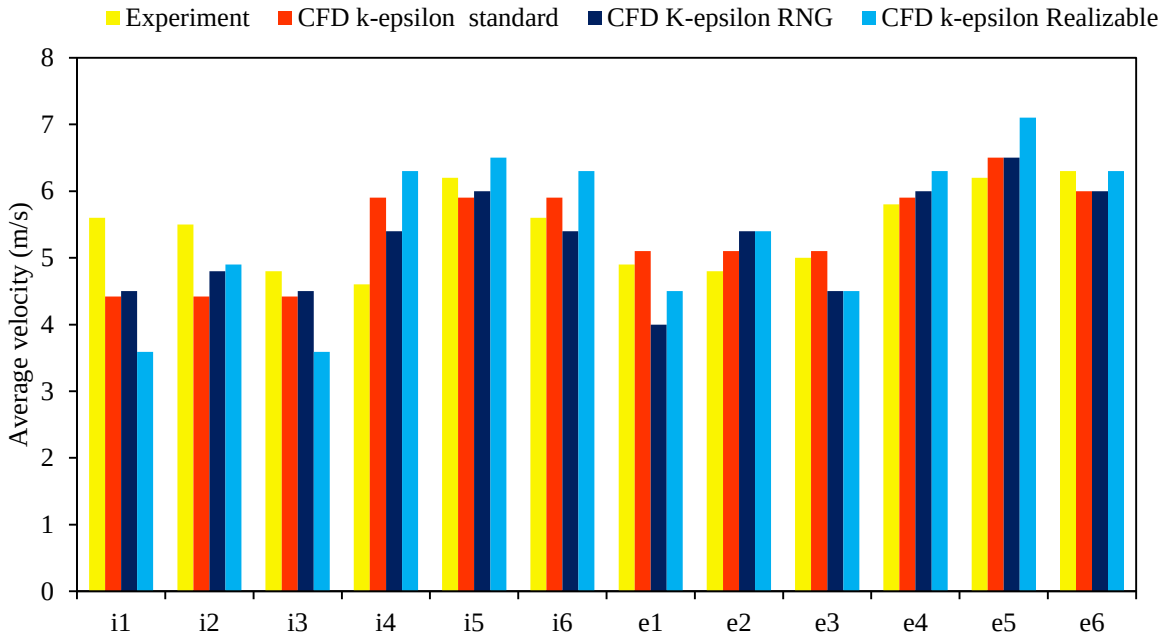

Figure 12. The impact of different turbulence models on the air velocity in supply and exhaust channel of 30° TWIW.

Table 3. The results of turbulence sensitivity analysis for 30° TWIW.

Point	Experiment	Sk-ε	RNG k-ε	Rk-ε
i1	5.6	4.42	4.5	3.59
i2	5.5	4.42	4.8	4.9
i3	4.8	4.42	4.5	3.59
i4	4.6	5.9	5.4	6.3
i5	6.2	5.9	6	6.5
i6	5.6	5.9	5.4	6.3
e1	4.9	5.1	4	4.5
e2	4.8	5.1	5.4	5.4
e3	5	5.1	4.5	4.5
e4	5.8	5.9	6	6.3
e5	6.2	6.5	6.5	7.1
e6	6.3	6	6	6.3
Average of difference with experiment	–	**11%**	**13%**	**18%**

4 Results and discussions

4.1 CFD validation with wind tunnel measurements

To validate the numerical method, the CFD results were compared against the experimental data obtained from wind tunnel testing of four reduced-scale models. Fig. 13, Fig. 14, Fig. 15 and Fig. 16 demonstrate the air velocity results obtained from experimental test and CFD simulation (measured in points I_1-E_6 of Fig. 6) related to TWIW 45°, 30°, 60° and CTSW model. It was found that the average percentage of error was 13.6%. Based on suggestion and justification of reference [42] and [43] it can be concluded that the validation procedure was satisfactory which proves the capability of CFD model to predict the flow behavior. As wall with small re-circulation at the opposite side, as the airflow was re-directed downwards observed in Fig. 13, Fig 14 and Fig 15, uneven airflow distribution can be seen between the inlet (I) points, but in general the airflow speed near the partition wall ($I_4 - I_6$) was higher as compared to the points closer to the opening of the wind catcher ($I_1 - I_3$). This was due to the 90 degree turn inside the supply channel of the wind catcher, causing the airflow to speed up near the partition into the room. While in the exhaust channel (E), the airflow near the partition wall (E_1-E3) was slower as compared to airflow near the exhaust opening (E_4-E6). Fig. 16 shows the CFD and experimental results for the analysis of the windcatcher with internal louvers at the openings.

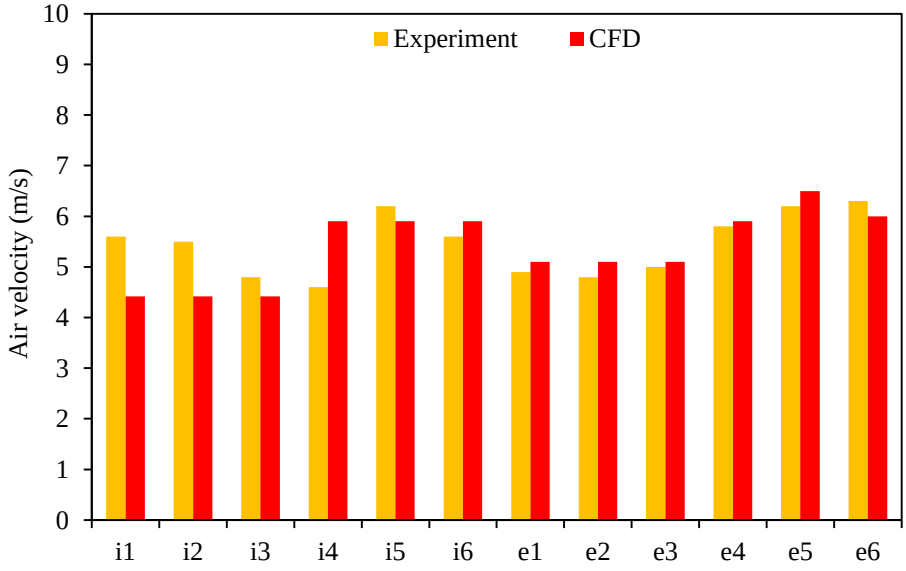

Figure 13. Comparison between experiment and CFD for the TWIW with 30° wing wall in 10 m/s wind speed.

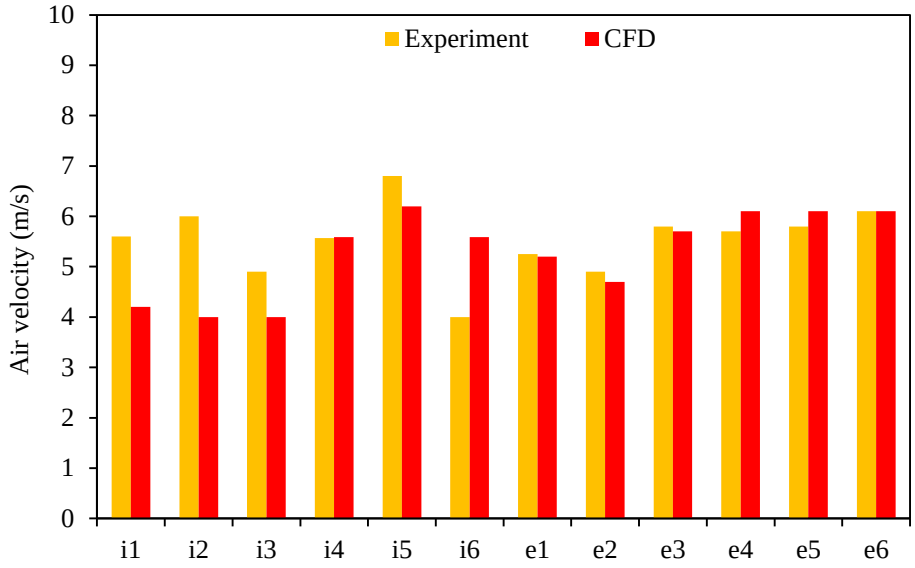

Figure 14. Comparison between experiment and CFD for the TWIW with 45° wing wall in 10 m/s wind speed.

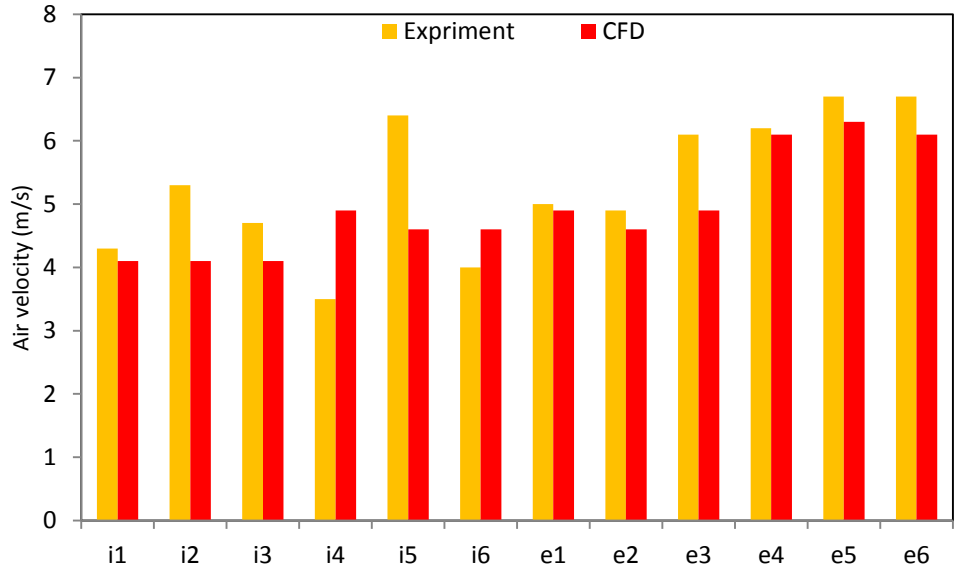

Figure 15. Comparison between experiment and CFD for the TWIW with 60° wing wall in 10 m/s wind speed.

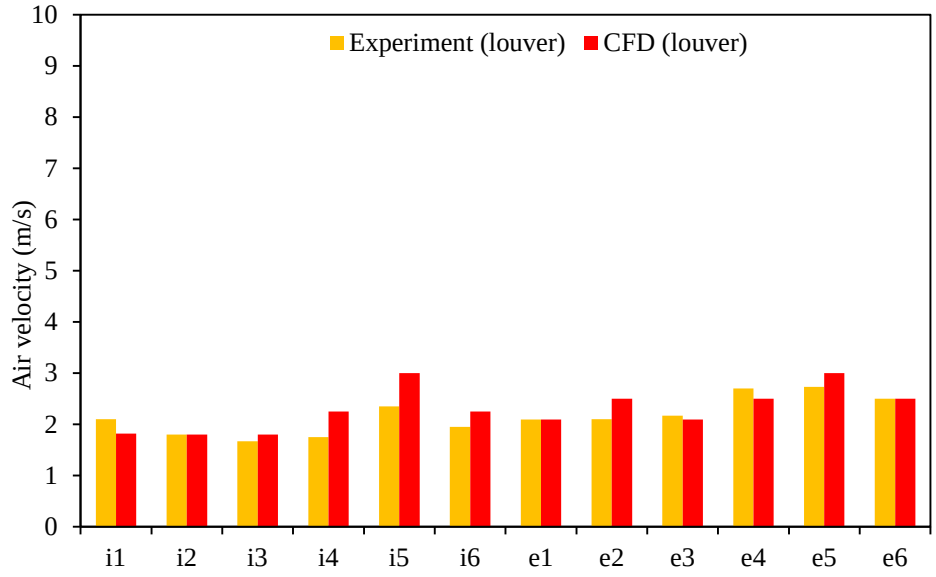

Figure 16. Comparison between experiment and CFD for the CTSW model in 10 m/s wind speed.

4.2 CFD simulation results

4.2.1 The effect of wing wall angle α on ventilation performance

To evaluate and compare the ventilation performance of different windcatcher configurations, the average of airflow velocity in the supply channel was analyzed; because it can demonstrates the ability of the windcatcher to provide fresh air into the building. This was carried out by drawing the plane (Fig. 17) inside inlet channels and calculating the average airflow velocity inside the plane.

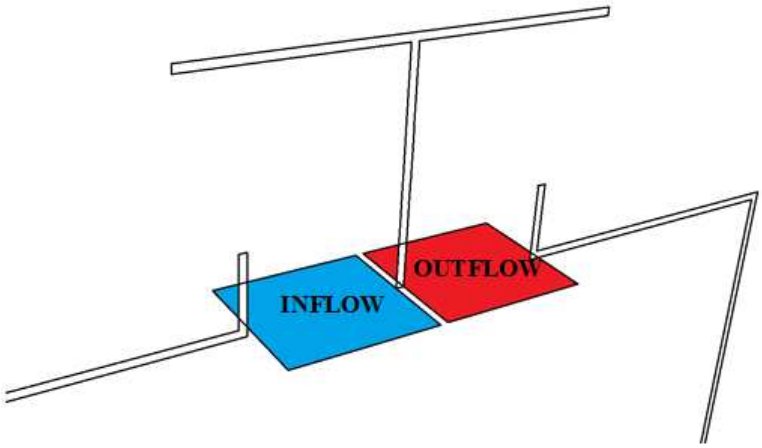

Figure 17. The diffusers in inlet channell and outlet channel where the air velocirty and air flow rate were clacluted.

Fig. 18 shows the CFD results of the ventilation performance of the windcatcher with different wing wall angles (5º to 70º) at increments of 5º.

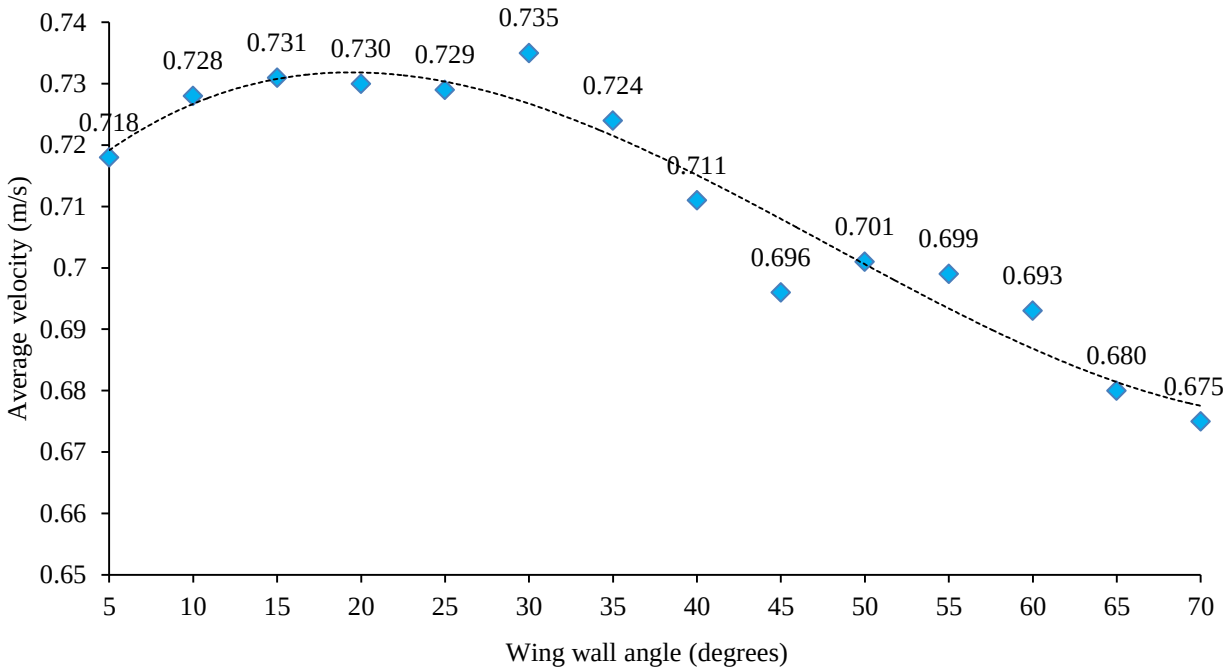

Figure 18. Effect of wing wall angle on supply air velocity in TWIW.

As observed in Fig. 18, the air velocity in the inflow was 0.718 m/s for the TWIW with 5° wing wall and gradually increases reaching maximum value 0.735 m/s at 30°. Next, a reductive trend was observed as the wing wall angle increases to 70° reaching the minimum value 0.68m/s which is 8.2% lower than 30°. With respect to the Fig. 18, the range of 15 to 30 degree represents the optimum angle for highest air velocity. The trend can be better explained by looking at the airflow pattern around the wing wall in the next figure which compares wing wall angle at 70º with 30º. As observed, the airflow was accelerated near the wing wall at 30º up to about 1 m/s and as a result it also increased the airflow speed inside the windcatcher. While for the wing wall at 70º, this acceleration in airflow speed was not observed and the speed measured at the same location was 0.78 m/s. In terms of outflow, the lower angle wing wall performed better as observed in the Fig. 19.

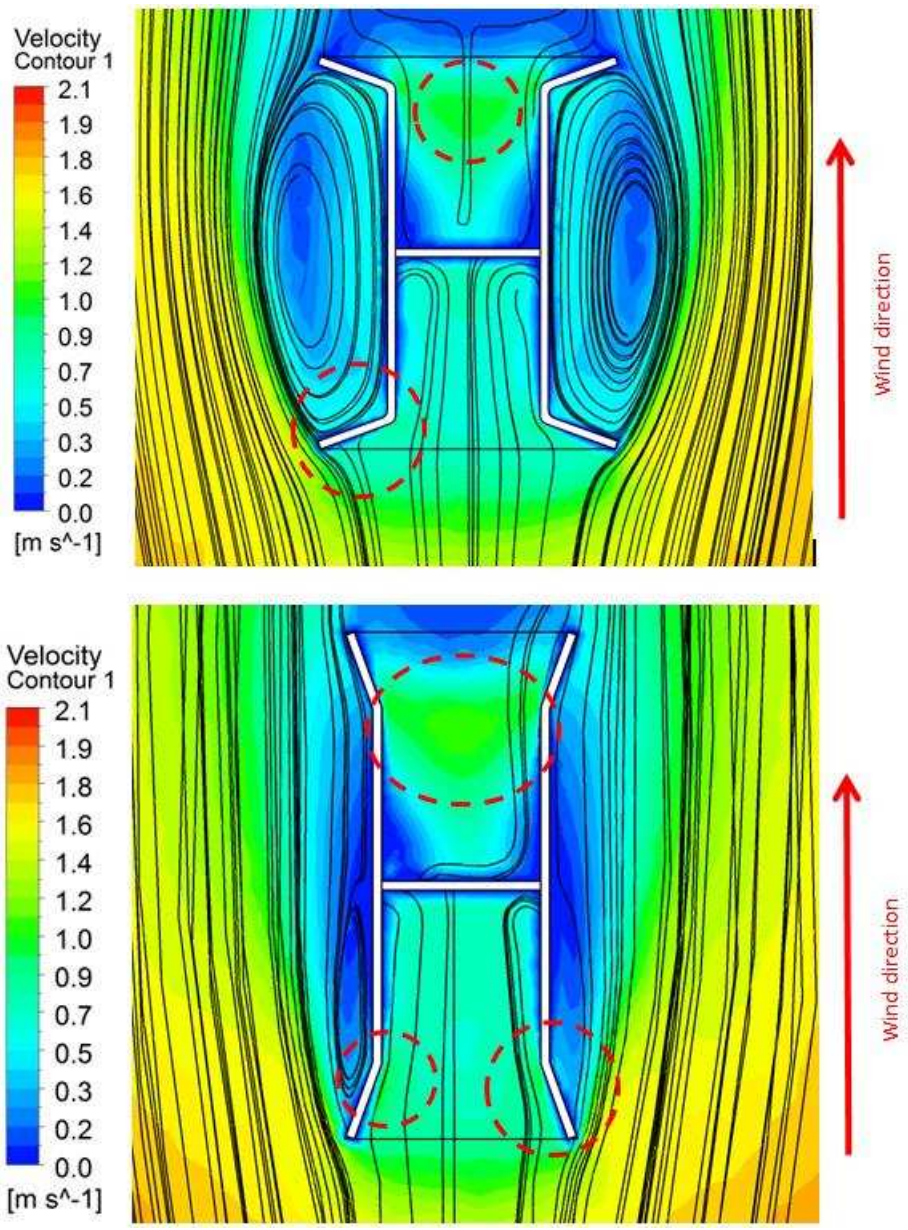

Figure 19. Comparison between the airflow in and around the 70° TWIW (top) and 30° TWIW (bottom).

4.2.2 Comparison between TWIW and CTSW

Fig. 20 shows the velocity contours of a cross-sectional plane inside the computational domain representing the airflow distribution inside the room with windcatcher integrated with 30º wing wall. As observed, the approach wind profile entered from the left side of the domain and the airflow slowed down as it approached the building and lifted up. Separation zones were observed on the front side of the building and front edge of the roof which affected the airflow entering the

windcatcher. The airflow inside the supply of the windcatcher was re-directed downwards when it hit the partition wall, causing the airflow to speed up near the partition wall reaching up to 1.2 m/s. The airflow induced inside the room spread as it reached the floor causing airflow recirculation on all sides. The average speed of the airflow inside the room was 0.152 m/s.

The airflow speed was significantly higher in the middle room hence a volume control system such as dampers is necessary to effectively distribute the airflow inside the space. This study did not include the effect of dampers, but Elmualim [44] and Hughes [34] had already investigated the topic in details. The airflow was recirculated inside the room and exited the space through the exhaust channel of the windcatcher; this was aided by the large airflow re-circulation generated at the back of the windcatcher and building model.

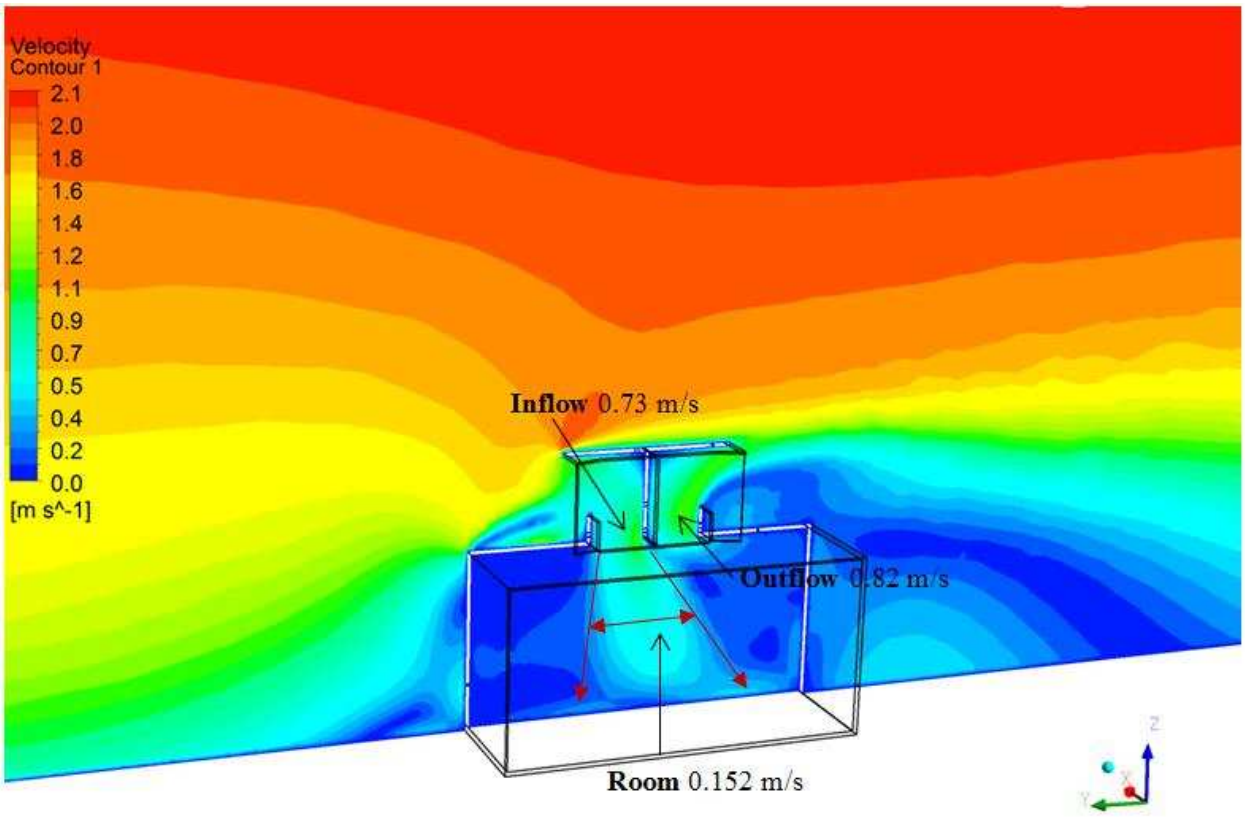

Figure 20. Velocity magnitude contours for the TWIW with 30º wing wall.

Fig. 21 presents the results of the airflow velocity distribution for the CTSW windcatcher with louvers in the openings. As compared to the previous model in Fig. 20, a similar flow profile was observed outside the building, except for the airflow at the back of the windcatcher which was

due to slower airflow velocity at the exit. Inside the windcatcher, significantly lower airflow speeds were observed and some recirculation flows were observed on one side of the channel which is a phenomenon also seen in previous windcatcher studies. Inside the room, a similar pattern was observed except for the airstream which was more concentrated at the middle of the room. The airflow exited the windcatcher at a much lower speed which was a result of the addition of the louvers in the exit opening.

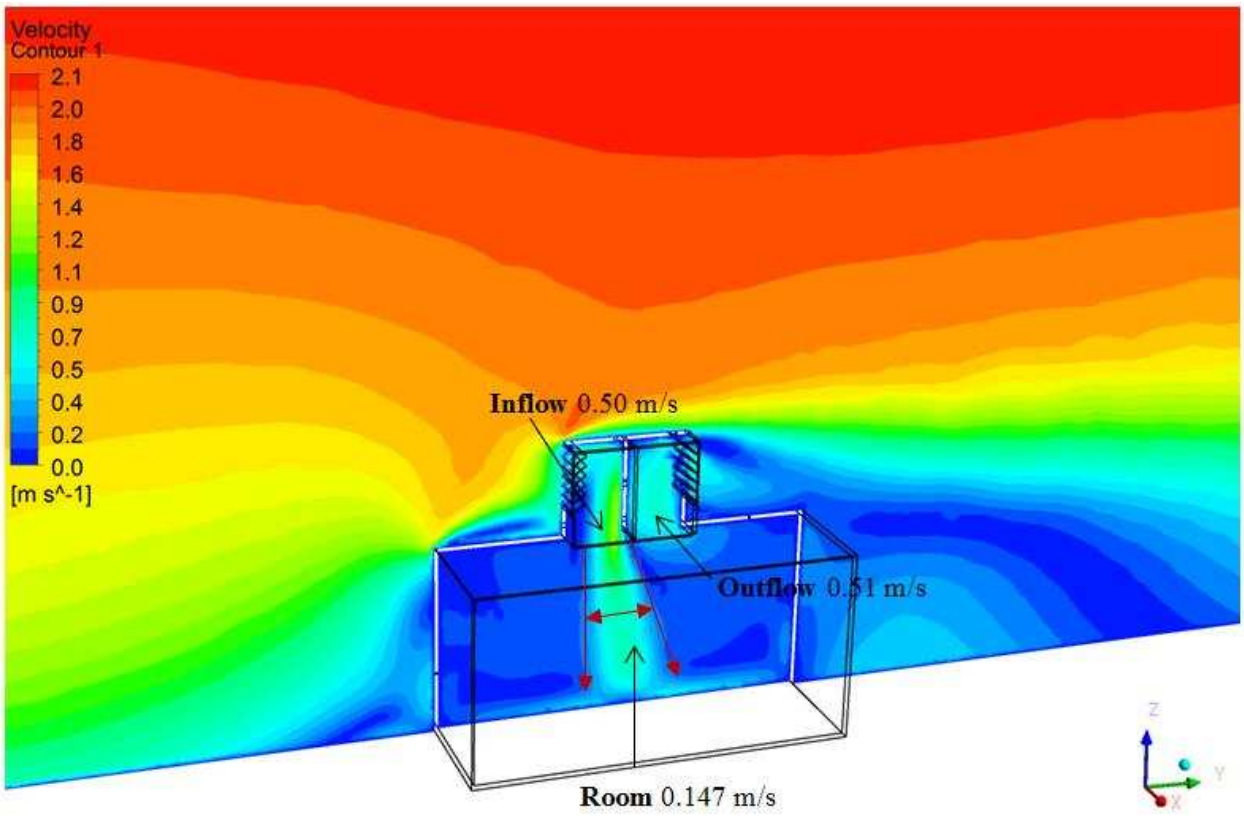

Figure 21. Velocity magnitude contours for the CTSW model.

Fig. 22 shows the total pressure contour of plane passing through the middle section of the windcatcher model with wing wall angled at 30º. The highest pressure around the windcatcher was observed in the corner of inlet channel with maximum value of 1.80 Pa Since the direction of flow is always from higher relative pressure zone to lower pressure zone, the lower pressure in room space (than the inlet) caused that flow to circulate inside the model. In addition, the sharp

edge of the room in upstream of the flow caused flow separation which resulted in considerable low pressure zone on the roof and in front of the inlet opening of the windcatcher. As the wind flows around the model, large air recirculation were observed at the back of the windcatcher and building model, which generated negative pressure in this areas ranging from -0.3 Pa to -0.1 Pa.

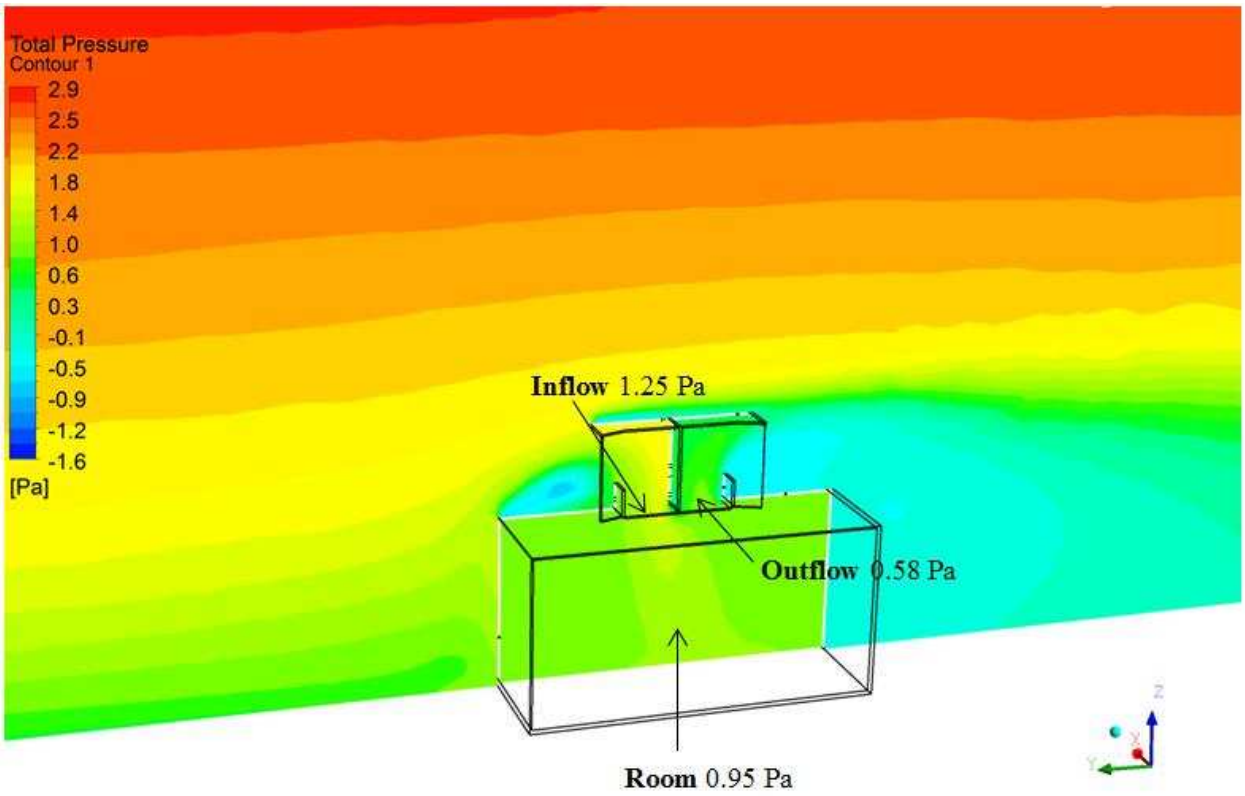

Figure 22. Total pressure contours for the TWIW with 30° wing wall.

Fig. 23 displays the contours for the CTSW model which have a lower average indoor pressure (0.39 Pa) as compared to the TWIW model (0.95 Pa).

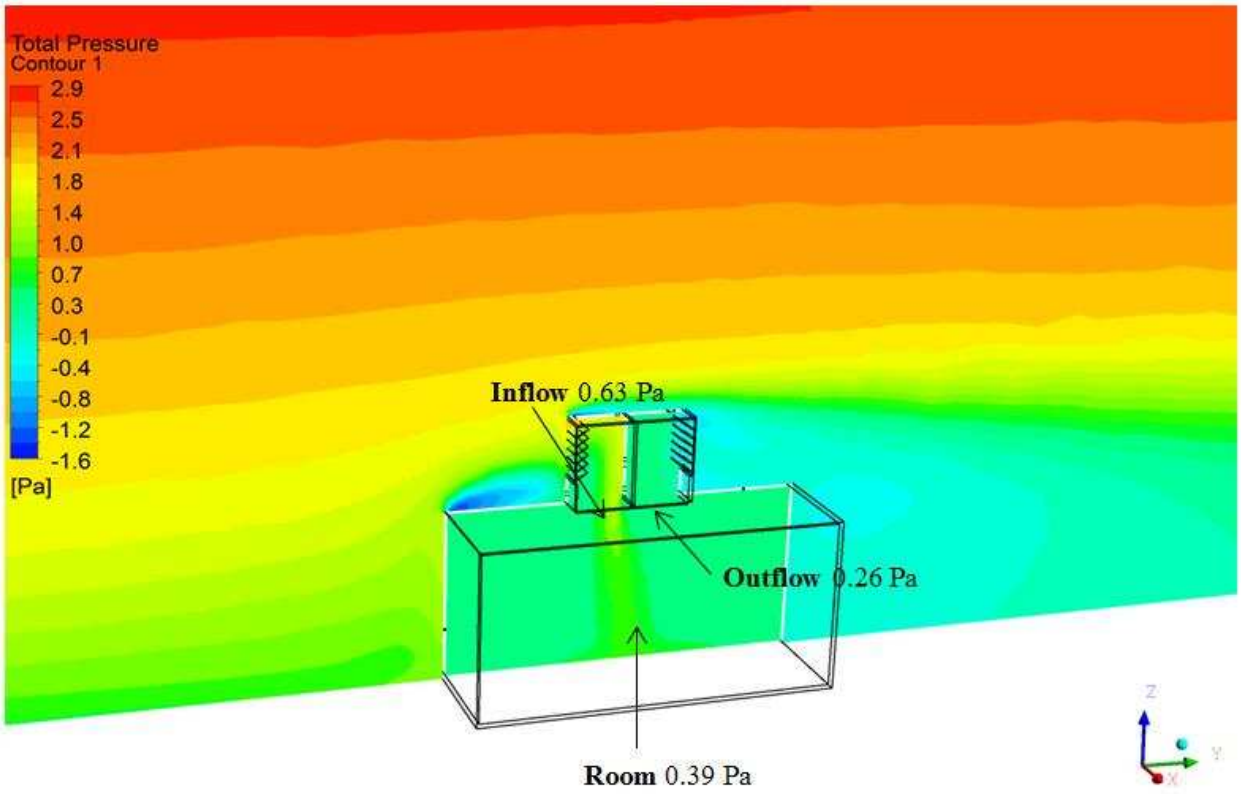

Figure 23. Total pressure contours for the CTSW model.

Apart from the air velocity improvement, the comparison between the TWIW 30° and CTSW model (Fig. 20 and Fig. 21) showed that the air velocity in TWIW channel had more uniform pattern than the CTSW. Therefore, the area with nearly zero speed was less observed in TWIW model. With respect to reference [9], this area are known as dead zones and is considered as a common problem in usual windcatcher that can reduce the ventilation efficiency of windcatcher. It can be easily seen in Fig 21 that that a big dead zone existed in the inlet channel of CTSW model while in inlet channel of TWIW was ignorable.

As it can be seen in Fig. 24 the zone with zero wind speed (or very close to zero) composed a considerable area of the channel in CTSW model. However, in TWIW the dead zone did not exist and air flow had smoother pattern when entering the room. The reason behind the dead zone can be explained by the presence of internal louvers. Although the size of the dead zone was increased in outlet channel of TWIW, it is still lower than CTSW model and the higher speed of air flow can offset it.

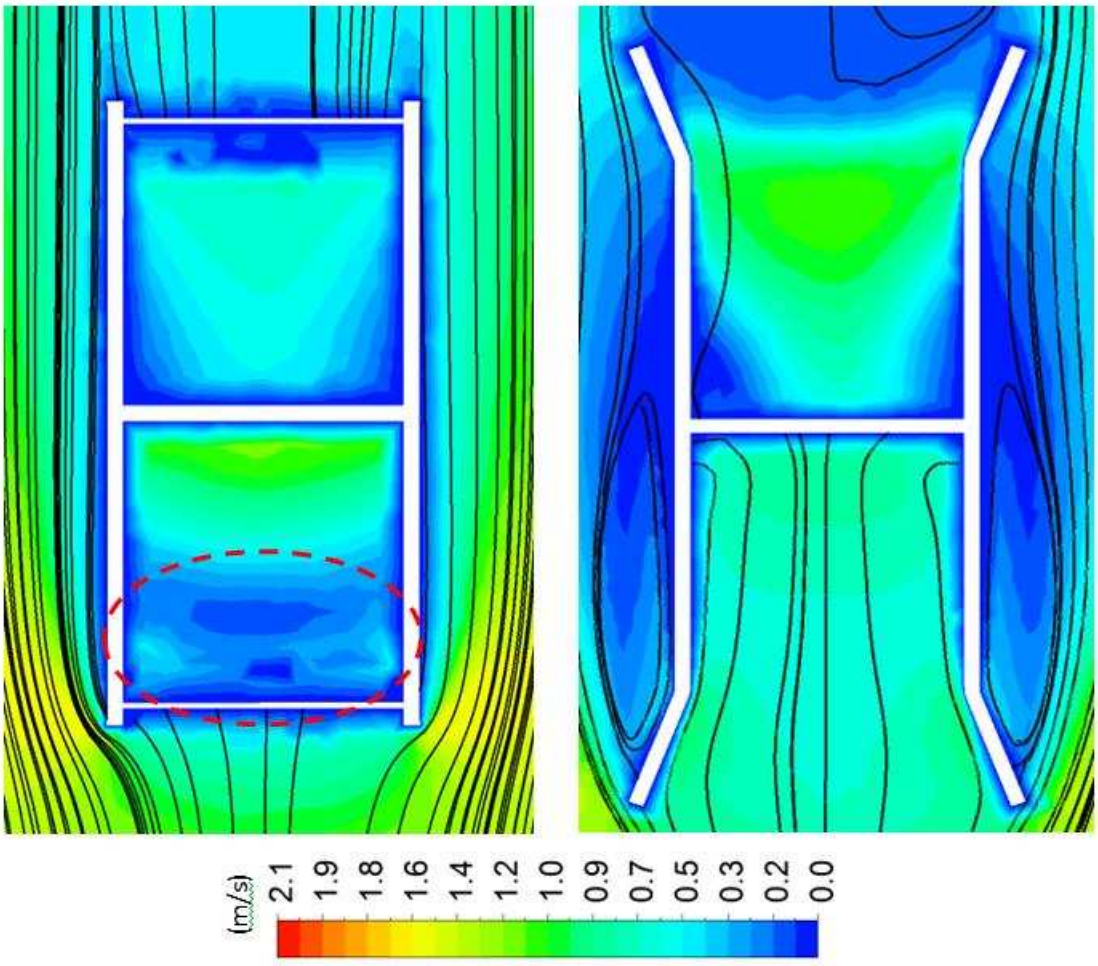

Figure 24. The comparison between air velocity in channel of CTSW (Left) and TWIW 30° (Right).

Fig. 25 shows a comparison between the total pressure inside and outside the channels of the windcatcher model with louvers and 30◦ wing wall, as observed, the airflow total pressure was reduced from 0.9Pa to 0.3Pa as it flowed inside the wind catcher with louvers. While for the TWIW, an increased from 0.8Pa to 1.2Pa was indicated.

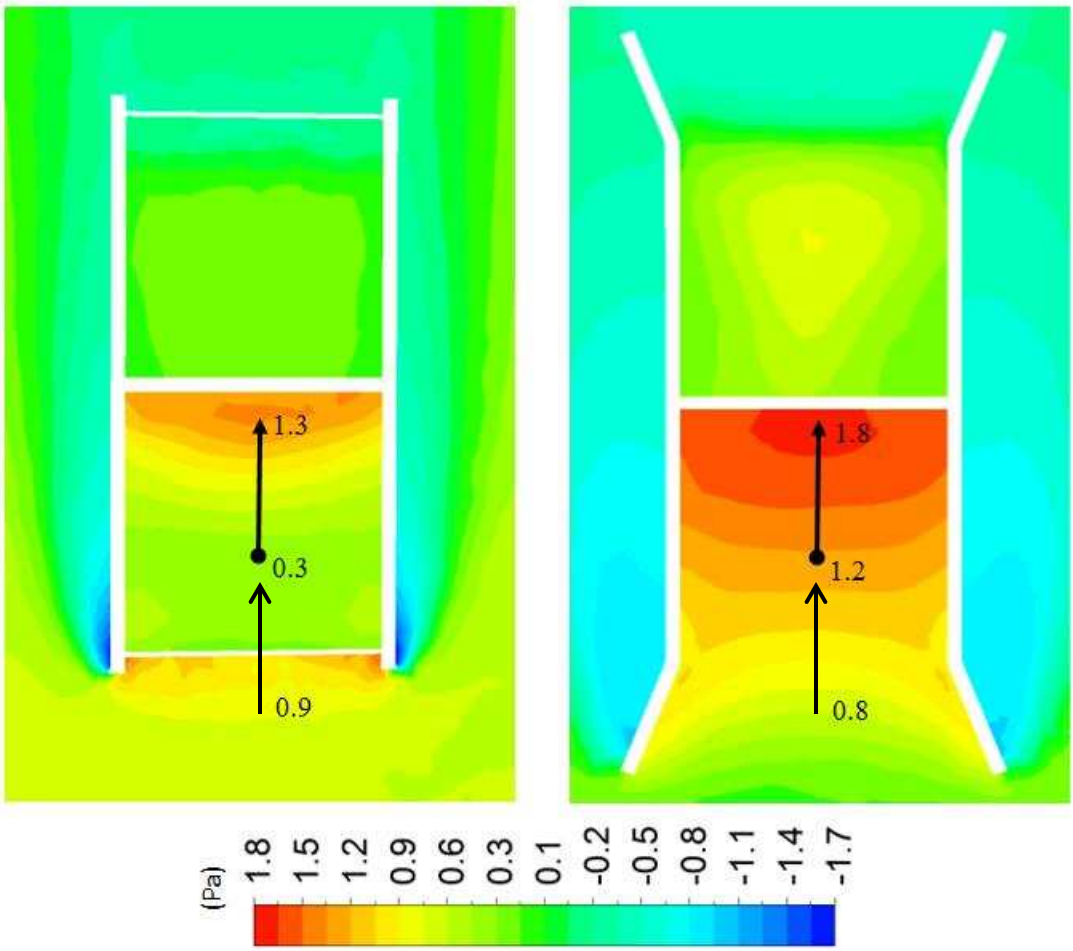

Figure 25. The comparison between total pressure in channel of CTSW and TWIW.

Fig. 26 demostrates the air flow velocity in supply diffuserin different outdoor wind speeds (0.5-2.5m/s). Comparison between TWIW and CTSW in different wind speeds showed that the airflow entering the the room with TWIWhad a speed of 36% of the outdoor wind speed, while in the CTSW model, the supplyair had only 24% of the outdoor wind speed. Thus, in same wind speed the TWIW could supply nearly 50% more fresh air than the CTSW.

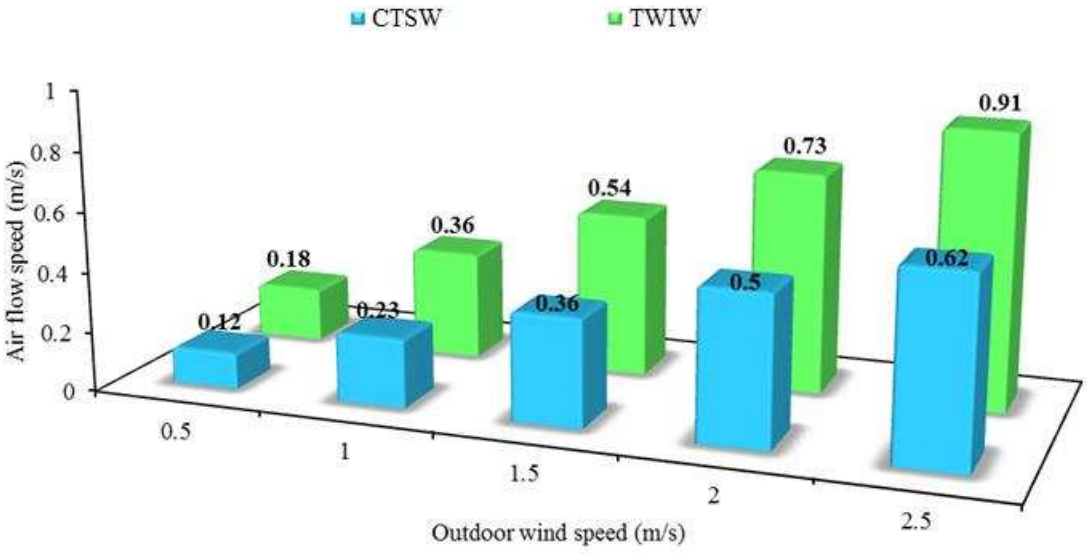

Figure 26. The air velocity in diffuser of TWIW and CTSW in different outdoor wind speeds.

4.2.3 Comparison of TWIW ventilation performance with standards

In ASHARE standard 62:2001 the minimum ventilation rate (V_R) is calculated base on following equation:

$$V_r=(A*O_d*R_p)+(A*R_a) \qquad \text{Equation 1}$$

In which O_d is the occupant density (persons per m^2), R_p is the required ventilation rate for each person (L/s per person),A is the area of ventilated space and R_a is the required ventilation rate for each square meter of the place (L/s /m^2). R_p and R_A can be selected for each type of ocupancy category (office .etc) in the ASHRAE standard 62.1 2007 [41]. If the model is supposed to represent a small classroom (A=24 m^2, R_P=3.8 L/s per person, R_A=0.3 L/s per m2, O_d=0.65 persons/ m^2), the minimum V_R will be:

$$(24*3.8*0.65)+(24*0.3)=68 \text{ L/s}$$

Comparing the air flow rate of TWIW with the minimum ASHRAE 62.1 2007 requirment in Fig. 27, reveals that it can easily supply at least three times more than standard requirment (even in low wind speed of 0.5 m/s) and increase in wind speed can lead to more air flow rate. At 2.5 m/s wind speed, TWIW can provide 900 L/s fresh air which was significantly much higher than

ASHRAE 62.1 2007 minumum requirment. This huge supply means that one TWIW can provide fresh air for bigger classroom area. Therefore, it can be concluded that TWIW can be very effective in low wind speed climate conditions and can rival convetional vetilation systems.

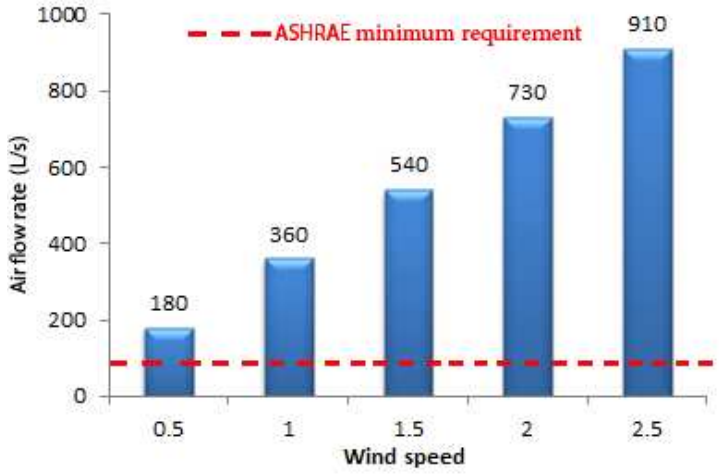

Figure 27. Comparing air flow rate of TWIW in different wind speed with minimum requirement of ASHRAE standard 62.1 2007 .

Comparing the capacity of TWIW with other types of windcatcher can better reveal its advantages. For instance, Haw et al. [21] reported that the ABS 500 windcatcher (a comercial product of Monodraught^{TM}) at 2 m/s wind speed can provide 30 L/s air flow rate. But, the TWIW can produce more than 730 L/s at same wind speed which is 24 times more than ABS 500.

In addition, another study conducted by Hughes and Gani [45] and [46] showed that the their four-sided windcatcher can provide 90 to 650 L/s air flow rate at wind speed of 1 to 5 m/s which was still lower than TWIW performance even in two times more outdoor speed. Another natural ventilation device named as Wing Jetter [10] which benefits from basic windcatcher concept, invented in Japan with a size of 1.5 m heightand 1.5 m width, can produce 110 L/s but in 6 m/s wind speed wich was also much lower than TWIW.

The next ventilation factor which was used to show the effectiveness of TWIW of was the air change rate. Air change rate also known as air changes per hour, (abbreviated as ACR or ACH) is a volume quantity of air enters or exits from a room which is divided by the room volume. In

other words, air changes rate shows how many times per hour, the air within a specific room is exchanged with fresh air. ACR is defined as below:

$$ACR = \frac{Q*3600}{V} \qquad \text{Equation 2}$$

Where Q is the volumetric flow rate and V is the volume of the room.

The ACH of TWIW in different wind speed was presented in Fig. 28. Haw et al. [21] in their field experiment examined a wind induced natural ventilation tower which also utilized basic concept of windcatcher. The obtained result for average ACH was 57 ACH in 3 m/s wind speed which was 25% more than TWIW but in higher wind speed and larger openingsize. In other field study conducted by Bansal et al. [47], the examined windcatcher achived 20 ACH at wind speed of 1 m/s which was slightly more than TWIW in that speed.

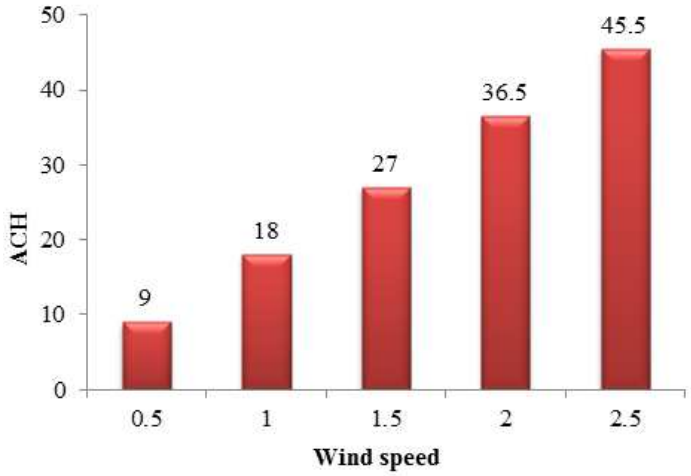

Figure 28. The Air Change Rate of TWIW in different wind speed.

5 Conclusion

Although windcatcher has a long history in Middle East and nowadays is utilized in other regions for natural ventilation, in some area with low ambient wind speed such as tropical countries there is serious hesitation to rely on it for ventilation. Wing wall as another natural ventilation strategy can potentially be integrated with windcatchers to improve its performance in

low wind speeds. Therefore, in this study the integration of two-sided windcatcher with wing wall was evaluated. The research consisted of experiment of reduced-scale models in wind tunnel and CFD simulation. Two types of computational domains were used in this study: one is for validating the numerical method using wind tunnel data and the other for simulating atmospheric boundary layer (ABL) flows around different types of windcatcher configurations. The approach flow profile considered obeyed the power law with an exponent of 0.25 which corresponds to a sub-urban terrain. The simulated airflow speeds were based on a low-wind speed conditions which ranged between 0.5-2.5 m/s. The experimental data were compared with the simulation results of four different configurations of the windcatcher model. A good agreement and trend was observed between the wind tunnel and CFD results. Different wing wall angles were examined by investigating the ventilation performance of the windcatcher with various angles (5º to 70º) at increments of 5º. The optimum angle range for the wing wall in terms of inflow was between 15º and 30º. The difference between optimum angle and 70º (as the minimum) was 8.2%. Comparison between TWIW and CTSW in different wind speeds showed that the speed of the airflow entering the the room with TWIW was of 36% of the outdoor wind speed while in the CTSW model, it was only 24%. Thus, in same wind speed the TWIW could supply nearly 50% more fresh air than the CTSW. Analysis of the airflow velocity contours showed that the TWIW model supplied a more evenly distributed airflow at the diffuser as compared to the CTSW model. In addition, the air streamline showed better pattern when entering the room and the dead zone region was ignorable in the TWIW. Comparing the performance of TWIW with ASHRAE standard demonstrated that even in low outdoor wind speed 0.5 m/s it can supply three times more than standard requirements. Likewise comparing TWIW with other types of windcatcher in previous studies revealed that it could supply similar or higher air flow rate and air change rate.

Acknowledgement

This research was conducted by ABER. The authors appriciate the Head of AEROLAB Prof. Dr. Wan Khairuddin bin Wan Ali and Engineer Abd Basid Abd Rahman as well as other staff for their kind copperation to conduct the experimental test.

Appendix I: Uncertainty Analysis

In order to evaluate the errors due to laboratory instruments, the analysis of uncertainties is needed. The investigated individual uncertainties, which are described below, proposed all of the errors which were caused by hotwires. The comprehensive explanation of presented method was explained by Kline and Mc Klintock [32].

- Uncertainty due to measuring by hotwire as mentioned in datasheet of OMEGA® HHF-SD1:

$$u_{h_A} = \frac{Measuring\ error}{\sqrt{3}} = \frac{0.01}{\sqrt{3}}$$

- Uncertainty of resolution digital display:

$$u_{h_R} = \frac{Resulation\ digital\ display \times 0.5}{\sqrt{3}} = \frac{0.01 \times 0.5}{\sqrt{3}}$$

- Uncertainty caused by repeated tests:

$$u_{h_n} = \frac{S_{T_i}}{\sqrt{n}}$$

$$S_{T_i} = \sqrt{\frac{\sum_{i=1}^{n}(V_i - \bar{V})^2}{n-1}}$$

$$\bar{V} = \frac{\sum_{i=1}^{n} V_i}{n}$$

- Final uncertainly:

$$u_h = \sqrt{{u_{h_A}}^2 + {u_{h_R}}^2 + {u_{h_n}}^2}$$

With the assumption of 95% are coverage for experiments, it could be concluded that K=2. So, the final uncertainly could be assumed as follow:

$$u = K \times u_h$$

$$u = 2 \times u_h$$

Based on mentioned calculations, the uncertainly of the experiments for inlet and outlet measurements were calculated. Fig. 30 presents the uncertainly analysis of TWIW with 30° angle in 10 m/s wind speed. As illustrated, the maximum uncertainly was less than 4.2%.

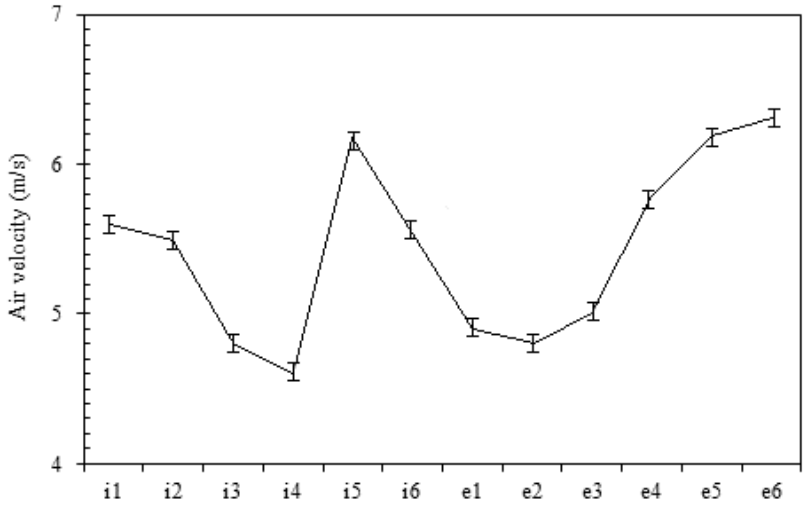

Figure 8. The uncertainly analysis of air velocity measurement of the inlet and outlet of 30° TWIW.

References

[1] J.K. Calautit, D. O'Connor, B.R. Hughes, A natural ventilation wind tower with heat pipe heat recovery for cold climates, Renewable Energy. (2015). doi:10.1016/j.renene.2015.08.026.

[2] J.K. Calautit, B.R. Hughes, Wind tunnel and CFD study of the natural ventilation performance of a commercial multi-directional wind tower, Building and Environment. 80 (2014) 71–83. doi:10.1016/j.buildenv.2014.05.022.

[3] T. Yu, P. Heiselberg, B. Lei, M. Pomianowski, C. Zhang, R. Jensen, Experimental investigation of cooling performance of a novel HVAC system combining natural ventilation with diffuse ceiling inlet and TABS, Energy and Buildings. 105 (2015) 165–177. doi:10.1016/j.enbuild.2015.07.039.

[4] H.M. Taleb, Natural Ventilation as Energy Efficient Solution for Achieving Low-Energy Houses in Dubai, Energy and Buildings. (2015). doi:10.1016/j.enbuild.2015.04.019.

[5] M. Afshin, A. Sohankar, M.D. Manshadi, M.K. Esfeh, An experimental study on the evaluation of natural ventilation performance of a two-sided wind-catcher for various wind angles, Renewable Energy. 85 (2016) 1068–1078. doi:10.1016/j.renene.2015.07.036.

[6] O. Saadatian, L.C. Haw, K. Sopian, M.Y. Sulaiman, Review of windcatcher technologies, Renewable and Sustainable Energy Reviews. 16 (2012) 1477–1495. doi:10.1016/j.rser.2011.11.037.

[7] H. Montazeri, Experimental and numerical study on natural ventilation performance of various multi-opening wind catchers, Building and Environment. 46 (2011) 370–378. doi:10.1016/j.buildenv.2010.07.031.

[8] A.R. Dehghani-sanij, M. Soltani, K. Raahemifar, A new design of wind tower for passive ventilation in buildings to reduce energy consumption in windy regions, Renewable and Sustainable Energy Reviews. 42 (2015) 182–195. doi:10.1016/j.rser.2014.10.018.

[9] A.A.A. Dehghan, M.K. Esfeh, M.D. Manshadi, Natural ventilation characteristics of one-sided wind catchers: experimental and analytical evaluation, Energy and Buildings. 61 (2013) 366–377. doi:10.1016/j.enbuild.2013.02.048.

[10] N. Khan, Y. Su, S.B. Riffat, A review on wind driven ventilation techniques, Energy and Buildings. 40 (2008) 1586–1604. doi:10.1016/j.enbuild.2008.02.015.

[11] B.R. Hughes, M. Cheuk-Ming, A study of wind and buoyancy driven flows through commercial wind towers, Energy and Buildings. 43 (2011) 1784–1791. doi:10.1016/j.enbuild.2011.03.022.

[12] M.N.N. Bahadori, M. Mazidi, a.R. Dehghani, A.R. Dehghani, Experimental investigation of new designs of wind towers, Renewable Energy. 33 (2008) 2273–2281. doi:10.1016/j.renene.2007.12.018.

[13] A.A. Elmualim, Integrated Building Management Systems for Sustainable Technologies: Design Aspiration and Operational Shortcoming, in: n.d.

[14] H. Montazeri, F. Montazeri, R. Azizian, S. Mostafavi, Two-sided wind catcher performance evaluation using experimental, numerical and analytical modeling, Renewable Energy. 35 (2010) 1424–1435. doi:10.1016/j.renene.2009.12.003.

[15] B.R. Hughes, J.K. Calautit, S.A. Ghani, The development of commercial wind towers for natural ventilation: A review, Applied Energy. 92 (2012) 606–627. doi:10.1016/j.apenergy.2011.11.066.

[16] C.C.C. Siew, a. I.I. Che-Ani, N.M.M. Tawil, N. a. G.A.G. Abdullah, M. Mohd-Tahir, Classification of Natural Ventilation Strategies in Optimizing Energy Consumption in Malaysian

Office Buildings, Procedia Engineering. 20 (2011) 363–371. doi:10.1016/j.proeng.2011.11.178.

[17] C.M. Mak, J.L. Niu, C.T. Lee, K.F. Chan, A numerical simulation of wing walls using computational fluid dynamics, Energy and Buildings. 39 (2007) 995–1002. doi:10.1016/j.enbuild.2006.10.012.

[18] T. Widodo, B. Riyadi, A parametric study of wind catcher model in a typical system of evaporative cooling tower Using CFD, Applied Mechanics and Materials. 660 (2014) 659–663. doi:10.4028/www.scientific.net/AMM.660.659.

[19] S. Liu, C.M. Mak, J. Niu, Numerical evaluation of louver configuration and ventilation strategies for the windcatcher system, Building and Environment. 46 (2011) 1600–1616. doi:10.1016/j.buildenv.2011.01.025.

[20] W. ZHIHONG, THE CONTROL OF AIRFLOW AND ACOUSTIC ENERGY FOR VENTILATION SYSTEM IN SUSTAINABLE BUILDING, The Hong Kong Polytechnic University, 2014.

[21] L.C. Haw, O. Saadatian, M.Y. Sulaiman, S. Mat, K. Sopian, Empirical study of a wind-induced natural ventilation tower under hot and humid climatic conditions, Energy and Buildings. 52 (2012) 28–38. doi:10.1016/j.enbuild.2012.05.016.

[22] B. Givoni, Man, climate and architecture, Elsevier, 1969.

[23] S. Chungloo, C. Tienchutima, The Effect of Wing-Walls and Balcony on Wind Induced Ventilation in High-Rise Residential Units, JARS. 8 (2011) 109–120.

[24] Q. Chen, Ventilation performance prediction for buildings: A method overview and recent applications, Building and Environment. 44 (2009) 848–858. doi:10.1016/j.buildenv.2008.05.025.

[25] Liliana Campos-Arriaga, Wind Energy in the Built Environment: A Design Analysis Using CFD and Wind Tunnel Modelling Approach, University of Nottingham, 2009.

[26] N. Khatami, The Wind-Catcher, A Traditional Solution For A Modern Problem, University of Glamorgan/ Prifysgol Morgannwg, 2009.

[27] J.K. Calautit, B.R. Hughes, H.N. Chaudhry, S.A. Ghani, CFD analysis of a heat transfer device integrated wind tower system for hot and dry climate, Applied Energy. 112 (2013) 576–591. doi:10.1016/j.apenergy.2013.01.021.

[28] B.R. Hughes, S. a a A. Ghani, A numerical investigation into the effect of Windvent louvre external angle on passive stack ventilation performance, Building and Environment. 45 (2010) 1025–1036. doi:10.1016/j.buildenv.2009.10.010.

[29] M.R. Islam, R. Saidur, N.A. Rahim, Assessment of wind energy potentiality at Kudat and Labuan, Malaysia using Weibull distribution function, Energy. 36 (2011) 985–992. doi:10.1016/j.energy.2010.12.011.

[30] K. Sopian, M.Y.H. Othman, A. Wirsat, The wind energy potential of Malaysia, Renewable Energy. 6 (1995) 1005–1016. doi:10.1016/0960-1481(95)00004-8.

[31] T.L. Tiang, D. Ishak, Technical review of wind energy potential as small-scale power generation sources in Penang Island Malaysia, Renewable and Sustainable Energy Reviews. 16 (2012) 3034–3042. doi:10.1016/j.rser.2012.02.032.

[32] S.J. Kline, F.A. McClintock, Describing uncertainties in single-sample experiments, Mechanical Engineering. 75 (1953) 3–8.

[33] J. Franke, A. Hellsten, H. Schlünzen, B. Carissimo, COST Action 732, Best Practice Guideline for the CFD Simulation of Flows in The Urban Environment, Brussels, 2007.

[34] B.R. Hughes, S.A.A. Abdul Ghani, A numerical investigation into the effect of windvent dampers on operating conditions, Building and Environment. 44 (2009) 237–248. doi:10.1016/j.buildenv.2008.02.012.

[35] A.A. Elmualim, Dynamic modelling of a wind catcher/tower turret for natural ventilation, Building Services Engineering Research and Technology. 27 (2006) 165–182. doi:10.1191/0143624406bse159oa.

[36] ANSYS Incorporated, ANSYS 14.5 FLUENT Theory Guide, (2015). http://www.ansys.com.

[37] Y. Tominaga, A. Mochida, R. Yoshie, H. Kataoka, T. Nozu, M. Yoshikawa, et al., AIJ guidelines for practical applications of CFD to pedestrian wind environment around buildings, Journal of Wind Engineering and Industrial Aerodynamics. 96 (2008) 1749–1761. doi:10.1016/j.jweia.2008.02.058.

[38] Y. Tominaga, S. Akabayashi, T. Kitahara, Y. Arinami, Air flow around isolated gable-roof buildings with different roof pitches: Wind tunnel experiments and CFD simulations, Building and Environment. 84 (2015) 204–213. doi:10.1016/j.buildenv.2014.11.012.

[39] B.E. Launder, D.B. Spalding, The numerical computation of turbulent flows, Computer Methods in Applied Mechanics and Engineering. 3 (1974) 269–289. doi:10.1016/0045-7825(74)90029-2.

[40] T. Cebeci, P. Bradshaw, Momentum transfer in boundary layers, Hemisphere Publishing Corp, New York, 1977.

[41] B. Blocken, T. Stathopoulos, J. Carmeliet, CFD simulation of the atmospheric boundary layer: wall function problems, Atmospheric Environment. 41 (2007) 238–252. doi:10.1016/j.atmosenv.2006.08.019.

[42] Z. Zhang, W. Zhang, Z.J. Zhai, Q.Y. Chen, Evaluation of Various Turbulence Models in Predicting Airflow and Turbulence in Enclosed Environments by CFD: Part 2—Comparison with Experimental Data from Literature, HVAC&R Research. 13 (2011) 871–886.

[43] J.K. Calautit, B.R. Hughes, Measurement and prediction of the indoor airflow in a room ventilated with a commercial wind tower, Energy and Buildings. 84 (2014) 367–377. doi:10.1016/j.enbuild.2014.08.015.

[44] Abbas Ali Elmualim, H.B. Awbi, Wind Tunnel and CFD Investigation of the Performance of "Windcatcher" Ventilation Systems, International Journal of Ventilation. 1 (2002) 53–64. http://www.ijovent.org/doi/abs/10.5555/ijov.2002.1.1.53.

[45] B.R. Hughes, S. a. a. A. Ghani, Investigation of a windvent passive ventilation device against current fresh air supply recommendations, Energy and Buildings. 40 (2008) 1651–1659. doi:10.1016/j.enbuild.2008.02.024.

[46] B.R. Hughes, S.A. Ghani, A numerical investigation into the feasibility of a passive-assisted natural ventilation stack device, International Journal of Sustainable Energy. 30 (2011) 193–211. doi:10.1080/1478646X.2010.503275.

[47] N.K. Bansal, R. Mathur, M.S. Bhandari, A study of solar chimney assisted wind tower system for natural ventilation in buildings, Building and Environment. 29 (1994) 495–500. doi:10.1016/0360-1323(94)90008-6.